renchyma and air trapping. The detection of elastolysis, as demonstrated on Elastica van Gieson staining, in the patient's tissues supports the presence of parenchymal destruction by ESS cells. Bronchiolitis and ensuing air trapping during cystic formations have been implicated in the pulmonary manifestations of Sjögren's syndrome and other diffuse cystic lung diseases (10). Morgan et al. reported the potential of an elastic recoil force from normal alveolar tissue around a demolished area to cause thin-walled cysts (11). This mechanism appears to support the finding that most cysts remained intact in our patient, although the cavitary lesions and nodules composed of ESS cells disappeared following the administration of MPA therapy. However, the disappearance of some cysts was noted, which indicates that the air trapping generated by proliferating ESS cells along small airways was dominant, whereas parenchymal damage, if any, was minimal in some cysts.

The optimal treatment for low-grade ESS with pulmonary metastasis has not been established as of yet. However, several case reports have been published regarding the efficacy of progesterone and aromatase inhibitors in the treatment of metastatic low-grade ESS (12-16), and the guidelines for uterine neoplasms proposed by the Japan Society of Gynecologic Oncology recommend the use of hormonal therapy, including progesterone and aromatase inhibitors, in cases of recurrent low-grade ESS (17). For such patients, the median overall survival from recurrence is 41 to 62 months (12-16). Our patient has responded very well to MPA therapy, tolerating the treatment well with no adverse events for approximately five years. During this time, no new metastatic lesions have been identified. Consistent with the findings of previous reports (12-16), MPA therapy should be the first-line therapy for pulmonary metastases of low-grade ESS.

In conclusion, our patient with pulmonary metastasis of low-grade ESS 11 years after hysterectomy and bilateral salpingo-oophorectomy, manifested cystic, nodular and cavitary lesions simultaneously. Each of these radiologic findings individually is known to reflect pulmonary metastasis of low-grade ESS; however, the coexistence of these imaging features should also be considered indicative of pulmonary metastasis of low-grade ESS in cases involving a past history of resection of "leiomyoma of the uterus."

The authors state that they have no Conflict of Interest (COI).

Acknowledgement

We thank Ms. Phyllis Minick for her excellent proofreading of our English writing.

References

1. Tavassoli FA, Devilee P. Eds. Pathology and Genetics of Tumours of the Breast and Female Genital Organs. World Health Organization Classification of Tumours. IARC Press, Lyon, 2003.
2. Feng W, Hua K, Gudlaugsson E, Yu Y, Zhou X, Baak JP. Prognostic indicators in WHO 2003 low-grade endometrial stromal sarcoma. Histopathology **62**: 675-687, 2013.
3. Leath CA 3rd, Huh WK, Hyde J Jr, et al. A multi-institutional review of outcomes of endometrial stromal sarcoma. Gynecol Oncol **105**: 630-634, 2007.
4. Aubry MC, Myers JL, Colby TV, Leslie KO, Tazelaar HD. Endometrial stromal sarcoma metastatic to the lung: a detailed analysis of 16 patients. Am J Surg Pathol **26**: 440-449, 2002.
5. Itoh T, Mochizuki M, Kumazaki S, Ishihara T, Fukayama M. Cystic pulmonary metastases of endometrial stromal sarcoma of the uterus, mimicking lymphangiomyomatosis: a case report with immunohistochemistry of HMB45. Pathol Int **47**: 725-729, 1997.
6. Kim GY, Sung CO, Han J, Park JO, Lee KS. Pulmonary metastases of uterine endometrial stromal sarcoma: diffuse micronodular and ground glass opacities: a case report. J Korean Med Sci **19**: 901-903, 2004.
7. Abrams J, Talcott J, Corson JM. Pulmonary metastases in patients with low-grade endometrial stromal sarcoma: clinicopathologic findings with immunohistochemical characterization. Am J Surg Pathol **13**: 133-140, 1989.
8. Inayama Y, Shoji A, Odagiri S, et al. Detection of pulmonary metastasis of low-grade endometrial stromal sarcoma 25 years after hysterectomy. Pathol Res Pract **196**: 129-134, 2000.
9. Gadkowski LB, Stout JE. Cavitary pulmonary disease. Clin Microbiol Rev **21**: 305-333, 2008.
10. Rowan C, Hansell DM, Renzoni E, et al. Diffuse cystic lung disease of unexplained cause with coexistent small airway disease: a possible causal relationship? Am J Surg Pathol **36**: 228-234, 2012.
11. Morgan MD, Edwards CW, Morris J, Matthews HR. Origin and behaviour of emphysematous bullae. Thorax **44**: 533-538, 1989.
12. Nakayama K, Ishikawa M, Nagai Y, Yaegashi N, Aoki Y, Miyazaki K. Prolonged long-term survival of low-grade endometrial stromal sarcoma patients with lung metastasis following treatment with medroxyprogesterone acetate. Int J Clin Oncol **15**: 179-183, 2010.
13. Pink D, Lindner T, Mrozek A, et al. Harm or benefit of hormonal treatment in metastatic low-grade endometrial stromal sarcoma: single center experience with 10 cases and review of the literature. Gynecol Oncol **101**: 464-469, 2006.
14. Lim MC, Lee S, Seo SS. Megestrol acetate therapy for advanced low-grade endometrial stromal sarcoma. Onkologie **33**: 260-262, 2010.
15. Mizuno M, Yatabe Y, Nawa A, Nakanishi T. Long-term medroxyprogesterone acetate therapy for low-grade endometrial stromal sarcoma. Int J Clin Oncol **17**: 348-354, 2012.
16. Alkasi O, Meinhold-Heerlein I, Zaki R, et al. Long-term disease-free survival after hormonal therapy of a patient with recurrent low grade endometrial stromal sarcoma: a case report. Arch Gynecol Obstet **279**: 57-60, 2009.
17. The Guideline for Uterine Neoplasms. 2009. Japan Society of Gynecologic Oncology, Ed. 2009: 174-176.

© 2014 The Japanese Society of Internal Medicine
http://www.naika.or.jp/imonline/index.html

Am J Physiol Lung Cell Mol Physiol 306: L996–L1005, 2014.
First published April 4, 2014; doi:10.1152/ajplung.00276.2013.

Genistein attenuates hypoxic pulmonary hypertension via enhanced nitric oxide signaling and the erythropoietin system

Sachiko Kuriyama, Yoshiteru Morio, Michie Toba, Tetsutaro Nagaoka, Fumiyuki Takahashi, Shin-ichiro Iwakami, Kuniaki Seyama, and Kazuhisa Takahashi

Department of Respiratory Medicine, Juntendo University Graduate School of Medicine, Tokyo, Japan

Submitted 1 October 2013; accepted in final form 31 March 2014

Kuriyama S, Morio Y, Toba M, Nagaoka T, Takahashi F, Iwakami S-i, Seyama K, Takahashi K. Genistein attenuates hypoxic pulmonary hypertension via enhanced nitric oxide signaling and the erythropoietin system. *Am J Physiol Lung Cell Mol Physiol* 306: L996–L1005, 2014. First published April 4, 2014; doi:10.1152/ajplung.00276.2013.—Upregulation of the erythropoietin (EPO)/EPO receptor (EPOR) system plays a protective role against chronic hypoxia-induced pulmonary hypertension (hypoxic PH) through enhancement of endothelial nitric oxide (NO)-mediated signaling. Genistein (Gen), a phytoestrogen, is considered to ameliorate NO-mediated signaling. We hypothesized that Gen attenuates and prevents hypoxic PH. In vivo, Sprague-Dawley rats raised in a hypobaric chamber were treated with Gen (60 mkg/kg) for 21 days. Pulmonary hemodynamics and vascular remodeling were ameliorated in Gen-treated hypoxic PH rats. Gen also restored cGMP levels and phosphorylated endothelial NO synthase (p-eNOS) at Ser^{1177} and p-Akt at Ser^{473} expression in the lungs. Additionally, Gen potentiated plasma EPO concentration and EPOR-positive endothelial cell counts. In experiments with hypoxic PH rats' isolated perfused lungs, Gen caused NO- and phosphatidylinositol 3-kinase (PI3K)/Akt-dependent vasodilation that reversed abnormal vasoconstriction. In vitro, a combination of EPO and Gen increased the p-eNOS and the EPOR expression in human umbilical vein endothelial cells under a hypoxic environment. Moreover, Gen potentiated the hypoxic increase in EPO production from human hepatoma cells. We conclude that Gen may be effective for the prevention of hypoxic PH through the improvement of PI3K/Akt-dependent, NO-mediated signaling in association with enhancement of the EPO/EPOR system.

pulmonary hypertension; genistein; erythropoietin; endothelial nitric oxide synthase; phosphatidylinositol 3-kinase

CHRONIC ALVEOLAR HYPOXIA IS likely to initiate hypoxic pulmonary vasoconstriction (32) and chronic structural remodeling of those vessels, possibly contributing to chronic hypoxia-induced pulmonary hypertension (hypoxic PH) (39). In fact, the presence of PH at diagnosis of respiratory diseases is considered a critical determinant of prognosis (2, 6). The endothelial dysfunction that accompanies hypoxic PH has been attributed to a decreased production and release of the endothelium-derived vasodilator, primary nitric oxide (NO) (21). NO is produced mostly by endothelial NO synthase (eNOS), and efficient production of NO requires the phosphorylation of eNOS (p-eNOS) at Ser^{1177} by serine/threonine kinase Akt, a downstream target of phosphatidylinositol 3-kinase (PI3K) (7, 11, 28). Although the expression of eNOS and production of NO declined in hypoxic PH patients (13, 14), the opposite condition—enhancement of NO production or preservation of eNOS expression, as well as phosphorylation—actually lessened the progress of hypoxic PH (29).

Hypoxic polycythemic responses to erythropoietin (EPO) have long been believed to raise pulmonary vascular resistance, leading to the development of PH and failure of the right heart. However, polycythemia did not augment the severity of hypoxic PH in some experiments with rats (30). Additionally, an important, protective role for the vascular EPO/EPO receptor (EPOR) system was found to offset insultus from chronic hypoxia and ischemia (37, 38). EPOR is expressed on cardiomyocytes, cardiac fibroblasts, endothelial cells, and vascular smooth muscle cells (22). The phosphorylation of EPOR generates a variety of signaling molecules, such as PI3K (10), which inhibit apoptosis, induce cell proliferation, and promote p-eNOS (1, 43). In vivo, EPO treatment beneficially reduced the severity of pulmonary vascular and cardiac remodeling of the subjects with experimental PH (31, 44). In endothelial cells, both EPO and hypoxia increased EPOR and eNOS expression (3). In addition, a combined treatment with EPO and sildenafil acted synergistically to restore endothelial function after hypoxic exposure (12). These results indicate that the EPO/EPOR system has potential as a new therapeutic agent by virtue of its ability to activate NO-mediated signaling in victims of hypoxic PH.

Genistein (Gen), a phytoestrogen derived from soybeans and tested in numerous studies, has been shown to have vasodilative and cardioprotective effects. Gen enhanced eNOS activity and NO-mediated vasorelaxation, not only in the systemic circulation (40) but also in pulmonary arteries, independently of any estrogen-mediated mechanism (18). In addition, we previously found that a 21-day treatment with Gen significantly attenuated the development of monocrotaline (MCT)-induced PH in rats, another model of PH, by restoring eNOS expression (16). Therefore, this study was designed to investigate whether treatment with Gen would attenuate hypoxic PH through amelioration of the EPO/EPOR system and NO-mediated signaling.

MATERIALS AND METHODS

Animals and exposure to chronic hypoxia. All experimental and surgical procedures were approved by the Institutional Committee for "Use and Care of Laboratory Animals in Juntendo University" (Hongo, Tokyo, Japan), in accordance with the U.S. National Institutes of Health "Guide for the Care and Use of Laboratory Animals." Experiments were performed with adult male Sprague-Dawley rats (200–250 g) obtained from Charles River Laboratories (Yokohama, Japan).

The pulmonary normotensive rats (the control group; NL) were housed at the ambient barometric pressure (760 mmHg). Chronically hypoxic pulmonary hypertensive rats (the experimental group; HL) were housed in a hypobaric chamber (barometric pressure, ~380 mmHg; inspired O_2 tension, ~76 mmHg), which was flushed contin-

Address for reprint requests and other correspondence: S. Kuriyama, Dept. of Respiratory Medicine, Juntendo Univ., Graduate School of Medicine, 2-1-1 Hongo, Bunkyo-ku, Tokyo, Japan (e-mail: skuriyam@juntendo.ac.jp).

1040-0605/14 Copyright © 2014 the American Physiological Society

uously with room air to prevent accumulation of CO_2, NH_3, and H_2O for a period of 21 days, as described previously (25).

Animal experimental protocols. For these studies, rats were randomly assigned to one of the following four groups ($n = 6-8$ animals in each group) to be administered either vehicle or Gen (60 mg/kg; Sigma Chemical, St. Louis, MO) (39): *1*) control animals raised in normoxia; *2*) Gen-treated animals raised in normoxia; *3*) control animals raised in chronic hypoxia; *4*) Gen-treated animals raised in chronic hypoxia. For treatment, Gen was dissolved in a mixture of DMSO (Sigma Chemical) and polyethylene glycol (PEG; Sigma Chemical). Rats were given subcutaneous injections of Gen or vehicle (100 μl of a mixture containing 1.25% DMSO and 98.75% PEG) daily throughout the experiments.

The efficacy of dietary Gen by gavage was also evaluated throughout the additional experiments. The Gen dosage of 60 mg/kg by gavage once/day was given to rats during hypoxic exposure for 3 wk. For comparison of the plasma concentrations of Gen between the control sample, subcutaneous and dietary delivery was examined by using the Gen TR-FIA (Labmaster, Aura, Finland) at the end of hypoxic exposure.

Hemodynamic measurements. Animals were anesthetized by intraperitoneal injection with pentobarbital sodium (15 mg/kg) and implanted with catheters in the pulmonary and right carotid arteries and right jugular vein, as described previously (16). Right ventricular systolic pressure (RVSP) and systemic arterial pressure (SAP) were measured with a polygraph system (AT-600G cardiotachometer; Nihon Kohden, Tokyo, Japan).

Measurement of RV hypertrophy. Each heart was dissected to assess the severity of PH. An index of RV hypertrophy was calculated as the ratio of wet weight of the RV wall to wet weight of the left ventricular (LV) wall plus septum (RV/LV + S).

Morphological studies. At the end of each hemodynamic study, the rats were killed with an overdose of pentobarbital sodium, and the thorax was opened. After blood samples were drawn from the right ventricle, the heart and lungs were removed en bloc. The trachea was intubated, and the left lung was inflated with 10% formalin at 36 cm H_2O pressure and fixed in the inflated state for 3 days. The right lung was frozen in liquid nitrogen for further molecular analysis.

Sections of pulmonary arteries were treated with elastic van Gieson stain for morphometric analysis of the arteries' medial-wall thickness to assess the degree of their muscularization, as described previously (16). In each tissue section, at least 50 consecutive arteries (>30 μm external diameter) were examined at ×400 magnification using an image analysis system (KS400; Carl Zeiss Imaging Solutions GmbH, Hallbergmoos, Germany). The medial-wall thickness was measured at two locations of each artery and calculated according to the following formula: (medial-wall thickness/external diameter) × 100 (in percent).

Pulmonary sections were also stained with EPOR antibody (1:50, anti-EPOR; Santa Cruz Biotechnology, Dallas, TX) to quantitate the EPOR immunoreactions. The paraffin-embedded, formalin-fixed lung specimens were washed and incubated with EPOR antibody overnight, followed by a 30-min incubation with the secondary antibody (1:300, biotinylated goat anti-rabbit IgG; Dako, Produktionsvej, Denmark). The color reaction was performed with 3,3-diaminobenzine. For quantitative analysis of the proportion of the EPOR immunoreaction, we counted the number of EPOR-positive endothelial cells of all endothelial cells in 50 consecutive pulmonary arteries within a size of 30–120 μm external diameter.

Vascular responses in isolated perfused lung. The rapid vasodilative effects of Gen were investigated in isolated perfused rat lungs, as described previously with minor modifications (24, 25). Lungs were harvested from NL and HL rats ($n = 6-8$ animals in each group) and ventilated with 21% O_2-5% CO_2-74% N_2 and perfused in a recirculating system. Effluent perfusate was drained from LV cannula into a perfusate reservoir, and the perfusate reservoir volume was monitored continuously. The perfusate was a physiological salt solution containing 116.3 mM NaCl, 5.4 mM KCl, 0.83 mM $MgSO_4$, 19.0 mM $NaHCO_3$, 1.04 mM NaH_2PO_4, 1.8 $CaCl_2$. 2 H_2O, and 5.5 mM D-glucose (Earle's balanced solution). Ficoll (4 g/100 ml, type 70; Pharmacia, Uppsala, Sweden) was included as a colloid. Before starting all experiments, 3.1 μmol/l sodium meclofenamate (Sigma Chemical) was added to inhibit synthesis of vasodilator prostaglandins (27, 36).

Initial experiments compared the vasoconstriction in responses to KCl (Sigma Chemical) of lungs from NL and HL rats. After equilibration, 5~20 mmol/l KCl was added to the perfusate in a concentration-response fashion every 5th min. Higher concentrations of KCl were not used because they caused lung edema. We next tested whether Gen has acute vasodilative effects against KCl-induced vasoconstriction in NL and chronic hypoxia lungs. At the peak of the KCl pressor response, 30 μmol/l Gen or vehicle (DMSO) was added to the perfusate. We also tested whether N^G-nitro-L-arginine (NLA; Sigma Chemical), an inhibitor of NOS, blocks the vasodilative response to Gen. NLA (200 μmol/l) was added to the perfusate at 20 min after administration of Gen or vehicle. Vascular effects were analyzed by measuring baseline perfusion pressure, peak KCl pressor response, the ratio of spontaneous (vehicle) or Gen-induced vasodilation to the KCl-induced vasoconstriction, and NLA-induced vasoconstriction. The ratio of vasodilation was calculated by dividing the decrease in pressure occurring from the addition of either vehicle or Gen to the perfusate at the peak of the KCl pressor response by the magnitude of the KCl pressor response.

To confirm further the mechanism in vascular responses to Gen, we examined whether the vasodilative effect of Gen was mediated by a PI3K/Akt-dependent pathway. LY294002, a specific PI3K inhibitor (10 μmol/l; Cayman Chemical, Ann Arbor, MI), was added to the perfusate at the peak of the KCl pressor response before the administration of Gen in separate experiments. Then, the alteration in vasodilative effect of Gen caused by the PI3K inhibitor was calculated as the ratio of vasodilation. To control for differences in vasoreactivity over time of perfusion, the inhibitor, antagonist, or respective vehicle was administrated identically with respective time.

cGMP measurement by enzyme immunoassay. cGMP levels in lung tissue were determined by the cGMP enzyme immunoassay (EIA; Cayman Chemical), according to the manufacturer's instructions, as described previously (20). The sample cGMP concentration was determined (as fmol/mg tissue) using the equation obtained from a standard curve. Each sample was evaluated in duplicate, and the process was repeated three times.

Western blots. Frozen lung tissues and pulmonary arteries were homogenized in lysis buffer containing 10 mM Tris-HCl, pH 7.6, 1 mM EDTA, 1% Triton X-100, and 1 mM protease inhibitor cocktail (Roche Diagnostics, Indianapolis, IN) using a tissue homogenizer. Samples were centrifuged for 15 min at 15,000 g at 4°C, and the supernatant protein concentration was estimated using a Micro BCA Protein Assay Reagent Kit (Pierce Biotechnology, Rockford, IL). Equal amounts of protein suspensions were separated electrophoretically on 5~10% SDS-polyacrylamide gels and transferred to polyvinylidene difluoride transfer membranes (GE Healthcare UK, Buckinghamshire, UK). Subsequently, the membranes were provided with anti-eNOS antibody (BD Biosciences, Franklin Lakes, NJ) or anti-p-eNOS (Ser^{1177}; Cell Signaling Technology, Danvers, MA). Signals were visualized by the ECL Prime detection system (Amersham Biosciences, GE Healthcare, Uppsala, Sweden). The protein bands were quantified using ImageJ software (version 1.43u).

Cells and cell culture. Human umbilical vein endothelial cells (HUVECs; Clonetics, Walkersville, MD) were cultured in 25-cm^2 flasks with a phenol red-free endothelial basal medium-2 (Lonza, Walkersville, MD) Bullet Kit, supplemented with endothelial growth medium 2 (Lonza, Basel, Switzerland) containing 5% FBS and cytokines. The human hepatoma cell line (HepG2; American Type Culture Collection, Manassas, VA) was cultured in DMEM containing 10% FBS. The medium was changed each day, and cells were

used within three to five passages. Cells were incubated under both 21% (normoxia) and 1% (hypoxia) oxygen for 48 h and were washed in HEPES buffer before exposure to hypoxia.

Combined treatment with Gen and EPO and protein analysis of HUVECs. HUVECs were cultured with the medium, which was replaced with or without 5 U/ml EPO and 10 μmol/l Gen for a 48-h exposure to the normoxia or hypoxia environment. Cells were washed and scraped from the plate, and the lysate was centrifuged for 15 min at 15,000 *g* at 4°C. The supernatant protein concentration was then estimated using a Micro BCA Protein Assay Reagent Kit (Pierce Biotechnology).

Measurement of EPO production in the culture supernatant of HepG2 cells under hypoxia. HepG2 cells were plated at a density of 5×10^5 cells/35 mm dish. At 24 h after the onset of culture, the medium was replaced with or without 10 μM Gen and then incubated for 48 h of exposure to normoxia or hypoxia. EPO protein concentration in the HepG2 cell culture supernatant was determined by chemiluminescent EIA by using Access EPO (Beckman Coulter, Brea, CA) as described previously (5).

Data analysis. Data are presented as means ± SE. Statistical analysis was done by unpaired *t*-test or one-way ANOVA, followed by Tukey's multiple comparisons test, or two-way ANOVA, followed by the Bonferroni test (Prism 5; GraphPad Software, San Diego, CA). Differences were considered significant at $P < 0.05$.

RESULTS

Treatment with Gen ameliorated hypoxic PH by restoring hemodynamics, preventing RV hypertrophy, and averting vascular remodeling. Exposure to conditions of chronic hypoxia caused severe PH; that is, HL rats had 50.6 ± 4.32 mmHg of peak RVSP compared with 9.6 ± 0.74 mmHg of peak RVSP in NL rats ($P < 0.05$, $n = 11{\sim}12$). Gen significantly attenuated the elevation of RVSP in HL rats but did not affect the peak RVSP in NL rats (Fig. 1*A*). SAP and heart rates (HR) were similar in all groups (Fig. 1, *B* and *C*). The severity of PH was confirmed further by RV hypertrophy (RV/LV + S); that

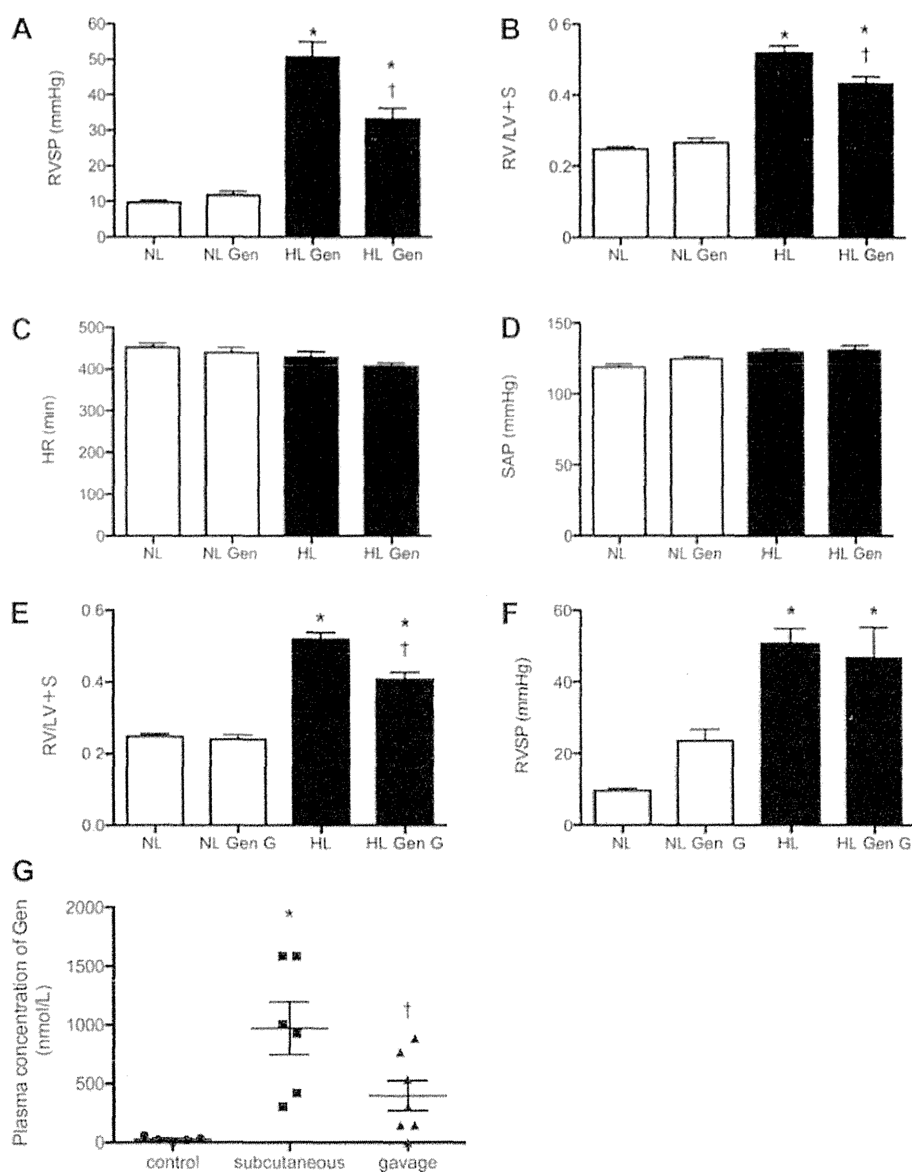

Fig. 1. Genistein (Gen) attenuated the chronic hypoxia-induced increases in (*A*) right ventricular systolic pressure (RVSP) and (*B*) RV hypertrophy [RV/left ventricular (LV) + septum (S)] of chronic hypoxia vehicle (HL) rats. However, Gen altered neither RVSP nor RV/LV + S in the normoxia vehicle (NL) group. Gen did not affect (*C*) heart rate (HR) or (*D*) systemic arterial pressure (SAP). Values are mean ± SE; $n = 11{\sim}12$ animals/group. $*P < 0.001$ vs. NL; $†P < 0.001$ vs. HL. *E*: dietary Gen by gavage (Gen G) attenuated the chronic hypoxia-induced increases in RV/LV + S but not (*F*) RVSP of HL rats. However, dietary Gen altered neither RVSP nor RV/LV + S in the NL group. Values are mean ± SE; $n = 5{\sim}6$ animals/group. $*P < 0.001$ vs. NL; $†P < 0.001$ vs. HL. *G*: the plasma concentration of Gen was lower in gavage than in subcutaneous delivery. Values are mean ± SE; $n = 5{\sim}7$ animals/group. $*P < 0.05$ vs. control; $†P < 0.05$ vs. subcutaneous.

is, the RV value of 0.52 ± 0.02 in HL rats was increased significantly over that of 0.25 ± 0.01 in NL rats ($P < 0.05$, n = 11~12). Gen diminished the increase in RV/LV + S in the HL bearers but did not affect their NL counterparts (Fig. 1*D*).

Dietary Gen by gavage also attenuated the magnitude of RV/LV + S but did not affect the elevation of RVSP in HL rats (Fig. 1, *E* and *F*). However, dietary Gen did not alter RVSP or RV/LV + S in the NL group. The plasma concentration was lower in gavage than in subcutaneous delivery (27.1 ± 21.2 nmol/l, 970.3 ± 549.7 nmol/l, and 398.2 ± 338.8 nmol/l, respectively, for control, subcutaneous, and gavage delivery; $P < 0.05$, n = 5–7/each group). The coefficient of variation of the concentrations were 77.9%, 56.7%, and 85.1%, respectively, for control, subcutaneous, and gavage delivery (Fig. 1*G*).

In the hypoxic condition, medial-wall thickness of muscular pulmonary arteries corresponding to terminal bronchioles was increased significantly when compared with that of NL animals. However, Gen treatment reduced the increase in medial-wall thickness of each vessel (vessel diameter of 30~60 μm, 60~120 μm, and >120 μm) in HL rats (Fig. 2, *A–D*).

Gen restores cGMP levels and preserves p-eNOS at Ser[1177] in hypoxic PH. To determine the cellular and molecular mechanisms used by Gen to lessen experimental hypoxic PH, we quantitated cGMP levels in lungs of all four groups used here. The cGMP levels in the whole lung were clearly lower in HL compared with NL tissues; comparatively, Gen preserved cGMP levels in lungs from the HL group. However, Gen increased cGMP levels slightly but not significantly in lungs from the NL group ($P < 0.05$, n = 6~8; Fig. 3*A*).

To examine the effects of Gen on eNOS and Akt activity, we assessed the p-eNOS at Ser[1177] and p-Akt at Ser[473] in lungs and pulmonary arteries. The representative Western blot analyses of lung homogenates are shown in Fig. 3, *B–E*. Although protein expression of eNOS or Akt, respectively, was increased or unaltered, the p-eNOS at Ser[1177] and p-Akt at Ser[473] decreased significantly in not only lungs but also pulmonary arteries from HL compared with NL rats. Gen attenuated the decrease in expression of p-eNOS but not p-Akt in the lungs manifesting HL but increased the expression of both p-eNOS and p-Akt in pulmonary arteries from the HL group. These

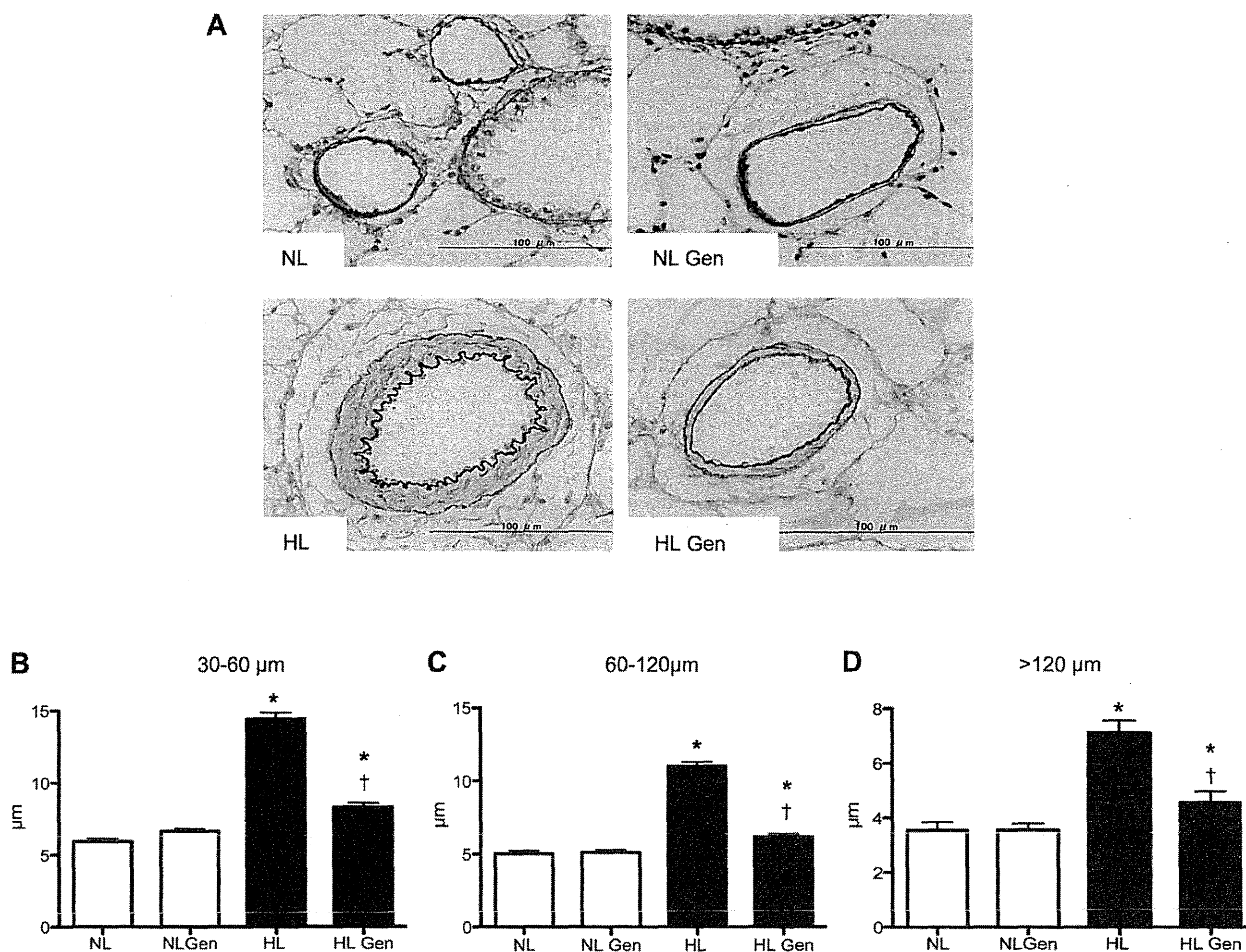

Fig. 2. Gen attenuated the chronic hypoxia-induced increase in medial-wall thickness of pulmonary arteries corresponding to terminal bronchioles (image of elastic van Gieson-stained section; *A*). *B*: vessel diameter of 30–60 μm; *C*: vessel diameter of 60–120 μm; *D*: vessel diameter of >120 μm. Values are mean ± SE; n = 5 animals/group. *$P < 0.001$ vs. NL; †$P < 0.001$ vs. HL.

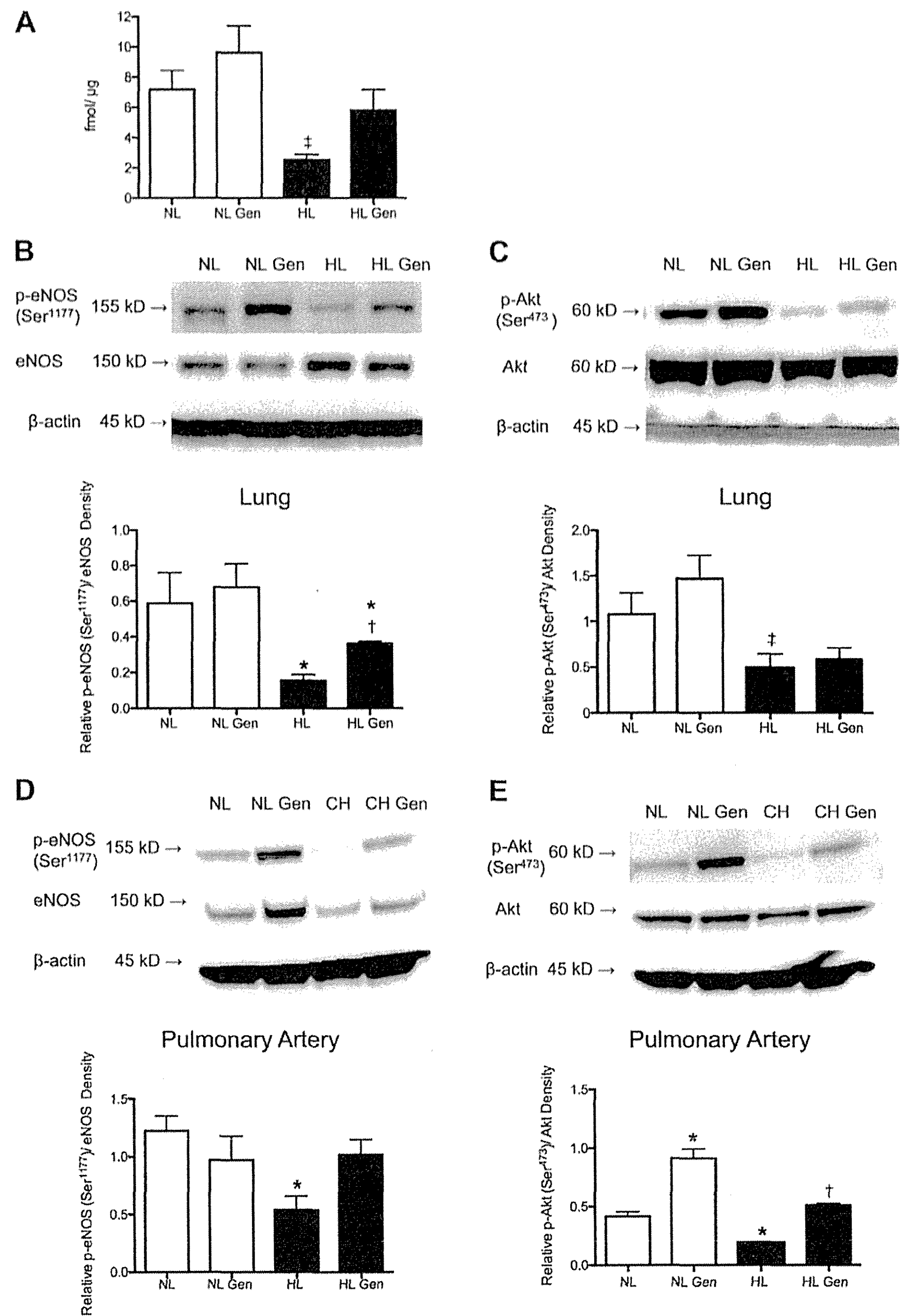

Fig. 3. Gen restored levels of both cGMP and phosphorylation of endothelial nitric oxide synthase (p-eNOS) at Ser^{1177} in lungs from HL rats. *A*: Gen restored a hypoxic decrease in cGMP levels in HL rats. Representative Western blots of protein in whole-lung homogenates for each group (respective *top*) and each densitometric quantification calculated as a percent of eNOS (*B*) or Akt protein (*C*; respective *bottom*). Although eNOS lost phosphorylation at Ser^{1177}, Gen restored p-eNOS at Ser^{1177} in lungs from HL rats. Representative Western blots of protein in pulmonary arteries from each group (respective *top*) and each densitometric quantification calculated as a percent of eNOS (*D*) or Akt protein (*E*; respective *bottom*). p-eNOS at Ser^{1177} and p-Akt at Ser^{473} were lost, but Gen restored p-eNOS at Ser^{1177} and p-Akt at Ser^{473} in pulmonary arteries from HL rats. Results were quantified in each of 4 experiments. Values are mean ± SE; n = 4–6 animals/group. *$P < 0.05$ vs. NL; †$P < 0.05$ vs. HL; ‡$P < 0.05$ vs. NL Gen.

results suggest that Gen restored the expression of both p-eNOS and p-Akt selectively in pulmonary arteries.

Gen causes rapid vasodilation in isolated perfused lungs from NL and HL rats. In preparation for analyses of vasoconstriction and dilation, baseline levels were established. In 12~16 animals/group, we noted that the perfusion pressure was higher in vessels from HL rats (7.93 ± 0.37 mmHg) than in NL rats (6.25 ± 0.28 mmHg; $P < 0.05$, n = 12~16). Subsequently, KCl caused a concentration-dependent vasoconstriction that was greater in the HL group compared with NL animals (Fig. 4*A*). These results suggested the presence of increased vascular tone and abnormal vasoconstriction in pulmonary vessels during the course of HL. However, in the presence of KCl-induced vasoconstriction, Gen caused a similar extent of vasodilation in NL and HL vessels (Fig. 4*B*).

Rapid vasodilative effect of Gen is abolished by either NLA or a specific PI3K/Akt kinase inhibitor. The effect of Gen-induced vasodilation on KCl-induced vasoconstriction was abolished completely after NLA administration into the lungs of NL and HL rats (Fig. 4*C*). Pretreatment with LY294002, a specific PI3K/Akt kinase inhibitor, blunted the vasodilative effect of Gen significantly in both the NL and HL (Fig. 4*D*).

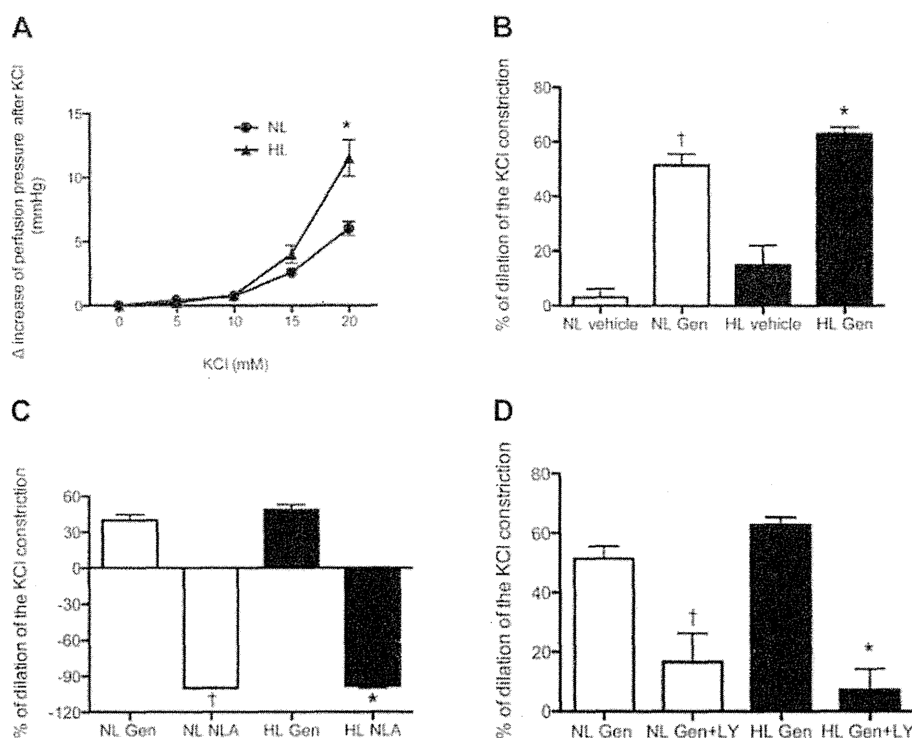

Fig. 4. *A*: concentration-dependent, cumulative effects of KCl on baseline perfusion pressure in NL and HL lungs. Values are mean ± SE; n = 12–16 animals/group. *$P < 0.05$ vs. NL. *B*: Gen caused similar vasodilation against KCl-induced vasoconstriction between NL and HL rat lungs. *$P <$ 0.05 vs. HL vehicle; †$P < 0.05$ vs. NL vehicle. *C*: the vasodilative effects of Gen on KCl-induced vasoconstriction were abolished completely by N^G-nitro-L-arginine (NLA) in NL and HL rat lungs. *D*: LY294002 (LY), a specific phosphatidylinositol 3-kinase inhibitor, blocked the vasodilative effect of Gen in lungs of both NL and HL rats. Values are mean ± SE; n = 6–8 animals/group. *$P <$ 0.05 vs. HL Gen; †$P < 0.05$ vs. NL Gen.

These results suggest that the mechanism of a Gen-induced vasodilative effect was dependent on eNOS but, at least in part, mediated through the PI3K/Akt pathway.

Gen increases hemoglobin concentration, hematocrit levels, EPO production, and EPOR-positive endothelial cell counts of pulmonary arteries in hypoxic PH. Prolonged exposure to a hypoxic condition caused a significant increase of the hemoglobin (Hb) concentration and hematocrit (Hct) levels (17.10 ± 1.50 g/dl and 51.30 ± 4.16%, respectively) in the HL group above that in NL subjects (13.24 ± 1.12 g/dl and 39.72 ± 3.81%, respectively; $P < 0.0001$, $n = 5–6$). Gen potentiated the hypoxic increase of Hb concentration and Hct levels (Fig. 5, *A* and *B*).

Similar to the rise in Hb concentrations and Hct levels, Gen potentiated the increases of serum EPO levels and percentages of EPOR-positive endothelial cells. That is, EPO was 18.98 ± 6.45 mU/ml for HL vs. 40.73 ± 14.82 mU/ml for HL Gen ($P <$ 0.05, $n = 8$), and percentages of EPOR-positive endothelial cell counts were 20.84 ± 7.38% for HL vs. 33.32 ± 6.06% for HL Gen ($P < 0.0001$, $n = 4–6$; Fig. 5, *C–E*). However, Gen did not affect Hb concentrations, Hct levels, EPO levels, or EPOR-positive endothelial cell counts in the NL groups.

EPO combined with Gen increases the p-eNOS at Ser[1177] and EPOR expression in HUVECs under hypoxic exposure. Since exogenous EPO (5 U/ml) and hypoxia (2% O_2) for 48 h increased expression of eNOS and EPOR in HUVECs (3), we examined whether Gen (10 μmol/l) would potentiate the p-eNOS at Ser[1177] and the expression of EPOR in cultured HUVECs for 48 h under 1% O_2 exposure with EPO (5 U/ml). Whereas 10 μmol/l Gen but not 5 U/ml EPO increased the p-eNOS at Ser[1177], the combined administration of EPO and Gen further potentiated the p-eNOS at Ser[1177] under hypoxic exposure (Fig. 6*A*). In addition, 10 μmol/l Gen alone and the combination of 10 μmol/l Gen and 5 U/ml EPO but not EPO alone upregulated EPOR protein expression, as shown by Western blot analysis in HUVECs under hypoxic exposure (Fig. 6*B*).

Hypoxia and Gen further increase EPO production in HepG2 cells. The human hepatoma cell lines, HepG2 and Hep3B, are widely used models for studying the production of EPO under hypoxic conditions. The mechanism is dependent on normal glycosylation of EPO, accumulation of cAMP, and interaction of cGMP and NO (26, 42). In our experiments, 1% O_2 exposure for 48 h induced a significant increase in EPO production in the culture medium from HepG2 cells compared with cells in a state of normoxia. Resulting values were 1.20 ± 0.00 mU/ml for normoxia vs. 5.57 ± 1.40 mU/ml for hypoxia ($P < 0.05$, $n = 4$). The addition of Gen (10 μmol/l) enhanced the production of EPO in HepG2 cells under hypoxic exposure (9.63 ± 2.37 mU/ml for hypoxia Gen vs. 5.57 ± 1.40 mU/ml for hypoxia; $P < 0.05$, $n = 4$; Fig. 6*C*). However, Gen did not affect EPOR expression in HUVECs or EPO production in HepG2 cells under normoxic exposure.

DISCUSSION

In the present study, we demonstrate clearly that Gen is capable of attenuating hypoxic PH by correcting its chronic structural remodeling component and also its abnormal vasoconstrictive component in the lungs. In addition, for the first time, we showed that the EPO/EPOR system and PI3K/Akt pathway are likely contributors to the ability of Gen to improve NO-mediated signaling.

In the pathogenesis of hypoxic PH, reduced NO-mediated vasodilation is a major factor in the impairment of endothelial-dependent vasodilation (15). This impaired vasodilation occurs

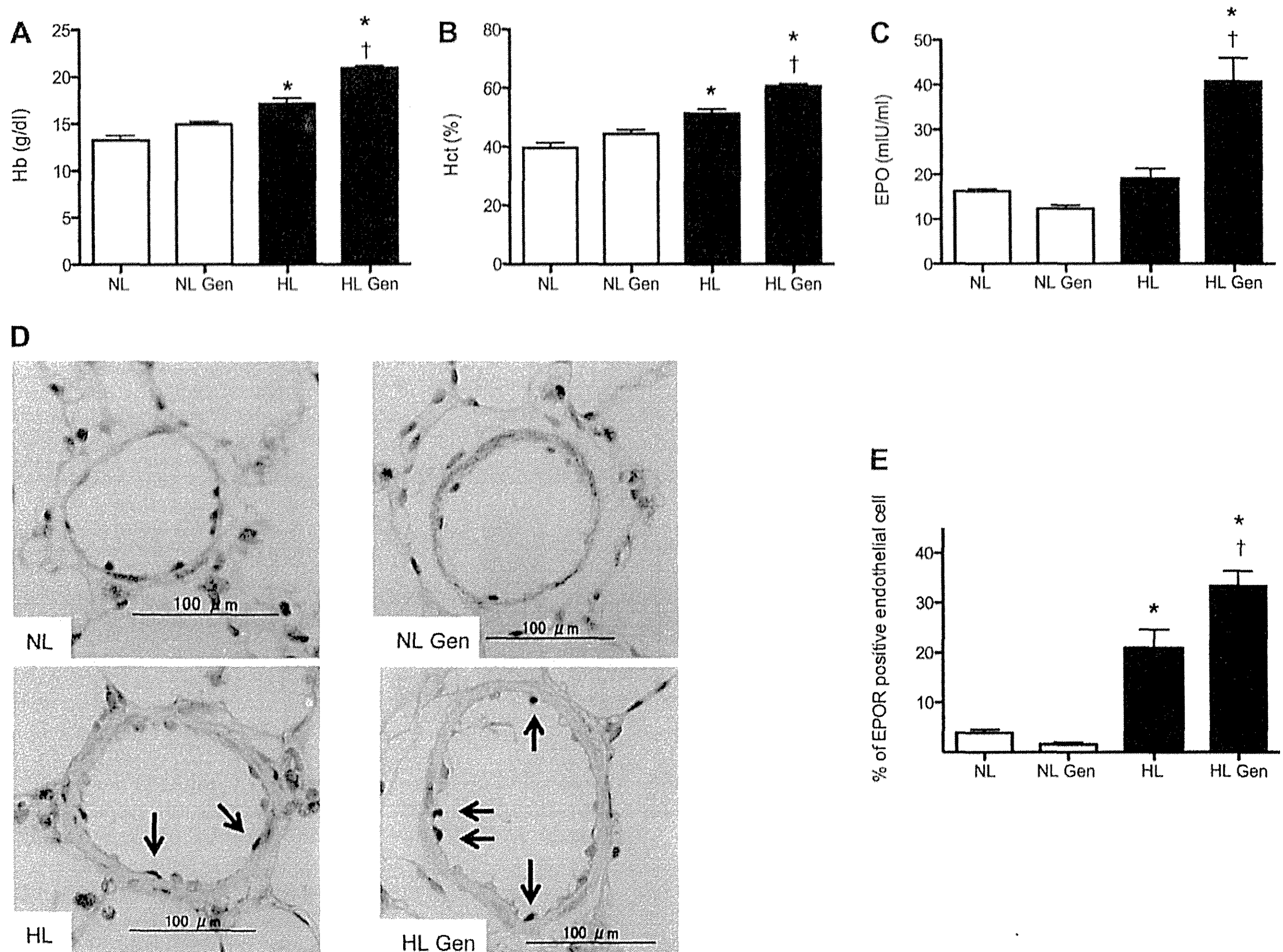

Fig. 5. Gen-upregulated chronic hypoxia-induced increases in (*A*) serum hemoglobin (Hb) and (*B*) serum hematocrit (Hct). Gen potentiated the chronic hypoxia-induced increases in serum erythropoietin (EPO) levels (*C*). Values are mean ± SE; n = 5~6 animals/group. $*P < 0.05$ vs. NL; $\dagger P < 0.05$ vs. HL. Representative microscopic images, immunohistochemical staining with the EPO receptor (EPOR) antibody, show localization of endothelial cells in pulmonary arteries from formalin-fixed, paraffin-embedded rat lung tissues (*D*) and percentages of EPOR-positive endothelial cells (*E*). *D*: arrows indicate the EPOR-positive endothelial cells. *E*: values are mean ± SE; n = 5~6 animals/group. $*P < 0.05$ vs. NL; $\dagger P < 0.05$ vs. HL.

in not only chronically hypoxic animal models but also patients with chronic obstructive lung disease and pulmonary arterial hypertension (4, 19). The defect in responsiveness to endothelium-dependent vasodilation is thought to be a consequence of reduced cGMP activity and of downstream NO production in hypoxic PH (8). In other words, the normalizing of NO-mediated signaling may contribute to attenuating hypoxic PH.

Chronic hypoxia-induced EPO production is a critical factor in the proliferation of red blood cells, and this response is traditionally believed to raise pulmonary vascular resistance, leading to the development of PH. In that context, the vascular EPO/EPOR system was recently invoked as a novel therapeutic target for cardiovascular disease (37). p-EPOR initiates a variety of signaling pathways, including PI3K, which is involved in NO-mediated signaling (23). In addition, in vivo studies showed that the effect of EPO on eNOS may be a physiologically relevant mechanism to counterbalance hypoxia (3).

The beneficial effects of Gen on cardiovascular diseases (9, 41) have been established and featured less toxicity and drug interactions than other treatments. Studies have shown that Gen interacted with vascular endothelial cells directly and increased NO production independently via an estrogen-mediated mechanism (31a, 45). We found that Gen significantly downregulated the development of MCT-induced PH by restoring eNOS expression in the lungs (16). These results indicate the strong potential of Gen as a therapeutic option for patients with hypoxic PH by virtue of its ability to mediate NO signaling and the EPO/EPOR system.

Long-term treatment with Gen restored normalcy to pulmonary hemodynamics and vascular remodeling, whereas a single dose of Gen produced rapid vasodilation to counterbalance vasoconstriction in this model. In experiments with isolated lungs perfused with a physiological salt solution, HL rats underwent elevations of baseline pressure, presumably produced by the increase in pulmonary resistance, resulting from vasoconstriction and vascular remodeling. In addition, the greater KCl pressor response of these HL animals indicated augmentation of abnormal vasoconstriction, probably caused

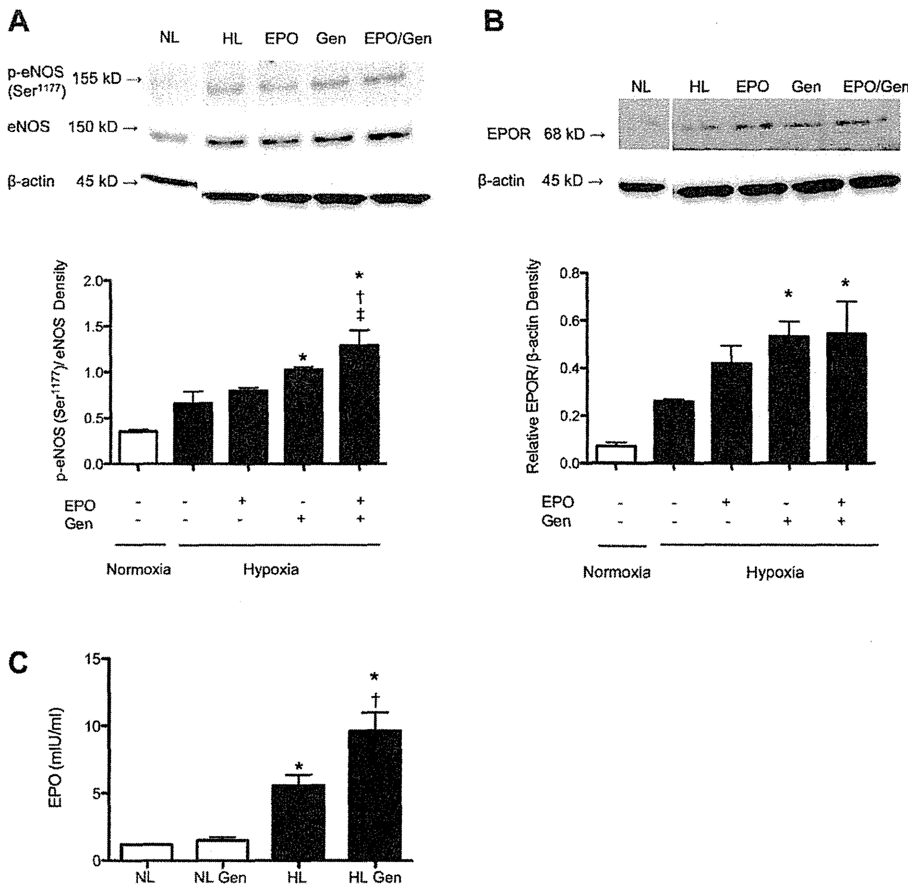

Fig. 6. *A*: representative Western blots of protein in p-eNOS at Ser[1177] of human umbilical vein endothelial cells (HUVECs) after 1% O_2 exposure for 48 h (*top*) and each densitometric quantification calculated as a percent of eNOS protein (*bottom*). Whereas 10 μmol/l Gen but not 5 U/ml EPO increased p-eNOS at Ser[1177], the combination of 5 U/ml EPO and 10 μmol/l Gen further potentiated the p-eNOS at Ser[1177] under hypoxic exposure. *B*: representative Western blots of protein in EPOR of HUVECs at 48 h of 1% O_2 exposure (*top*) and each densitometric quantification calculated as a percent of β-actin protein (*bottom*). Both 10 μmol/l of Gen alone and the combination of 10 μmol/l of Gen and 5 U/ml of EPO, but not EPO alone, increased the expression of EPOR under hypoxic exposure. Values are mean ± SE. $*P < 0.05$ vs. normoxia; $\dagger P < 0.05$ vs. hypoxia vehicle; $\ddagger P < 0.05$ vs. hypoxia EPO. *C*: hypoxia increased EPO production, and 10 μmol/l Gen then potentiated the hypoxic increase of EPO production in the human hepatoma cell line (HepG2 cells) in all of the triplicate experiments. Values are mean ± SE. $*P < 0.05$ vs. normoxia; $\dagger P < 0.05$ vs. hypoxia vehicle.

by boosting vascular tone in subjects exposed long-term to a low-oxygen environment.

Gen administered directly into the isolated perfused lung yielded a virtually immediate vasodilative effect that offset the abnormal augmentation of vascular tone in HL lungs. Since Gen-induced vasodilation was reduced by the NOS and PI3K inhibitors, apparently such vasodilation is dependent on PI3K/Akt- and NO-mediated signaling.

The present study showed that Gen suppressed the elevation of RVSP without causing systemic hypotension, reduced the HR, and prevented vascular remodeling in whole pulmonary arteries. It is generally agreed that the exacerbation of right heart failure caused by the elevation of RVSP and the systemic hypotension occurring after a decrease in cardiac output predispose PH patients to a fatal outcome. Because Gen did not affect the systemic blood pressure or the HR, Gen is a potentially useful agent for the prevention and treatment of hypoxic PH.

Mechanisms of Gen in preventing PH. We found that Gen restored levels of cGMP and p-eNOS at Ser[1177] and p-Akt at Ser[473] in hypoxic lungs and pulmonary arteries. The protein kinase Akt has been proposed to phosphorylate eNOS at Ser[1177] and to increase eNOS activity in response to various stimuli in vascular endothelial cells (7), whereas Gen activated eNOS through a PI3K/Akt-dependent mechanism in pulmonary arterial endothelial cells (45). For the first time, however, the present study of HL rats demonstrated that Gen treatment upregulated the PI3K/Akt pathway in the lungs and pulmonary arteries. Since the vasodilative effect of Gen was abolished by administration of a NOS or PI3K/Akt inhibitor in isolated perfused lungs, Gen treatment may be attributable to the improvement of NO-mediated signaling, mostly through an Akt-dependent mechanism. In fact, Gen restored the p-eNOS at Ser[1177] and p-Akt at Ser[473] in hypoxic lungs manifesting PH and pulmonary arteries from HL rats.

Here, Gen treatment enabled an increase in Hb concentration and Hct levels in association with upregulation of EPO in serum and EPOR expression in endothelial cells of pulmonary arteries. The mechanism of action of Gen in pulmonary vasculature may function through the EPO/EPOR system. In vitro, 10 μmol/l Gen increased the p-eNOS at Ser[1177] and EPOR expression in hypoxic HUVECs, as well as the production of EPO in hypoxic HepG2 cells. With the consideration of these results, Gen treatment may improve eNOS activities and upgrade the EPO/EPOR system, even though hypoxia is present.

Although our results raise the possibility that eNOS and the EPO/EPOR system are needed to improve each other under Gen treatment, the precise mechanism of their interaction is still unclear. The interaction of NO and cGMP is one of the pathways of hypoxia-induced stimulation of EPO gene expression (26). Administration of NLA, a NOS inhibitor, inhibited EPO production, although pretreatment with L-arginine prevented the inhibition (17). Whereas EPO increased eNOS transcription and activity through phosphorylation at Ser[1177]

(3), transgenic mice overexpressing EPO produced increased amounts of eNOS activity (34). Since that observation is compatible with ours, the present study suggests that Gen may be effective in promoting the EPO/EPOR system, thereby ameliorating the interaction between EPO and eNOS.

Limitations. There are limitations of this study. First, in isolated perfused lung experiments, we used a Hb-free physiological saline solution for perfusate. It has the possibility that the half-life of circulating NO is able to prolong and that the decreased clearance of NO may enhance the dilator response to Gen. Second, although the PH model demonstrated several main features of hypoxic PH, such as vascular remodeling and endothelial dysfunction, no plexiform lesions were seen, which is a hallmark feature of vasculature in pulmonary arterial hypertension and fatal PH patients, in the present study. Third, the cardiac output was not estimated directly as hemodynamic measurements. Although Gen demonstrated no obvious effects on systemic blood pressure and HR, we cannot exclude a possibility that decreased cardiac output may contribute to the reduction of RVSP. Fourth, in in vitro studies, HUVECs and the HepG2 cell line did not necessarily accord with pulmonary arterial endothelial cells because of some difference of property between them. Fifth, the present study did not delineate the exact relationship between the increase in p-Akt at Ser^{473} and p-eNOS at Ser^{1177}. Finally, the efficacy of Gen by other delivery, for example, dietary or inhalation, should be examined, because subcutaneous delivery was not necessarily pertinent. There raises a possibility of Gen as a promising option for treatment of hypoxic PH, since dietary Gen also attenuated RV hypertrophy of HL animals. However, contrary to subcutaneous delivery, dietary Gen did not affect the elevation of RVSP of HL animals. Although the reason of discrepancy was unclear, the lower and more inconsistent plasma concentration of dietary Gen may account for the different effects between subcutaneous and dietary delivery. On the other hand, as gut absorption and metabolism influenced large individual variation of plasma concentrations of Gen (33), suitable delivery of dietary Gen could answer these concerns. Further studies are required to elucidate these questions.

Conclusions. In the pathogenesis of hypoxic PH, endothelial cell dysfunction, characterized by the impairment of NO-mediated signaling, has been suggested to provoke abnormal vasoconstriction and vascular remodeling. Enhancement of the EPO/EPOR system in hypoxic conditions is thought to be a purposeful alteration that ameliorates endothelial function through upregulation of NO-mediated signaling. Our present study demonstrated for the first time that Gen, a phytoestrogen derived from soybeans, attenuated hypoxic PH by preventing vasoconstriction and chronic structural remodeling through restoration of NO-mediated signaling. In addition, Gen treatment enhanced the EPO/EPOR system function in the lungs and endothelial cells of pulmonary arteries from subjects with hypoxic PH. From these cumulative results, we envision that Gen may orchestrate the restoration of PI3K/Akt-dependent, NO-mediated signaling and enhancement of EPO/EPOR function, thereby preventing hypoxic PH. Based on our results and previous studies, combined with further examination and clinical studies, we propose that Gen may be an effective and safe option for the treatment of patients with hypoxic PH.

ACKNOWLEDGMENTS

We thank Etsuko Kobayashi for special technical assistance and Phyllis Minick for excellent proofreading.

DISCLOSURES

The authors declare no conflict of interest.

AUTHOR CONTRIBUTIONS

Author contributions: S.K., Y.M., M.T., T.N., F.T., K.S., and K.T. conception and design of research; S.K., Y.M., T.N., F.T., and S-i.I. performed experiments; S.K., Y.M., and S-i.I. analyzed data; S.K., Y.M., M.T., F.T., K.S., and K.T. interpreted results of experiments; S.K. and Y.M. prepared figures; S.K., Y.M., and K.T. drafted manuscript; S.K., Y.M., S-i.I., and K.T. edited and revised manuscript; S.K. and Y.M. approved final version of manuscript.

REFERENCES

1. **Akimoto T, Kusano E, Inaba T, Iimura O, Takahashi H, Ikeda H, Ito C, Ando Y, Ozawa K, Asano Y.** Erythropoietin regulates vascular smooth muscle cell apoptosis by a phosphatidylinositol 3 kinase-dependent pathway. *Kidney Int* 58: 269–282, 2000.
2. **Barberà JA, Peinado VI, Santos S.** Pulmonary hypertension in chronic obstructive pulmonary disease. *Eur Respir J* 21: 892–905, 2003.
3. **Beleslin-Cokic BB, Cokic VP, Yu X, Weksler BB, Schechter AN, Noguchi CT.** Erythropoietin and hypoxia stimulate erythropoietin receptor and nitric oxide production by endothelial cells. *Blood* 104: 2073–2080, 2004.
4. **Brett SJ, Simon J, Gibbs R, Pepper JR, Evans TW.** Impairment of endothelium-dependent pulmonary vasodilation in patients with primary pulmonary hypertension. *Thorax* 51: 89–91, 1996.
5. **Brugnara C.** Iron deficiency and erythropoiesis: new diagnostic approaches. *Clin Chem* 49: 1573–1578, 2003.
6. **Cottin V, Nunes H, Brillet PY, Delaval P, Devouassoux G, Tillie-Leblond I, Israel-Biet D, Court-Fortune I, Valeyre D, Cordier JF, Groupe d'Etude et de Recherche sur les Maladies Orphelines Pulmonaires (GERM O P).** Combined pulmonary fibrosis and emphysema: a distinct underrecognised entity. *Eur Respir J* 26: 586–593, 2005.
7. **Dimmeler S, Fleming I, Fisslthaler B, Hermann C, Busse R, Zeiher AM.** Activation of nitric oxide synthase in endothelial cells by Akt-dependent phosphorylation. *Nature* 399: 601–605, 1999.
8. **Fike CD, Kaplowitz MR, Thomas CJ, Nelin LD.** Chronic hypoxia decreases nitric oxide production and endothelial nitric oxide synthase in newborn pig lungs. *Am J Physiol Lung Cell Mol Physiol* 274: L517–L526, 1998.
9. **Filipeanu CM, Brailoiu E, Huhurez G, Slatineanu S, Baltatu O, Branisteanu DD.** Multiple effects of tyrosine kinase inhibitors on vascular smooth muscle contraction. *Eur J Pharmacol* 281: 29–35, 1995.
10. **Fisher JW.** Erythropoietin: physiology and pharmacology update. *Exp Biol Med (Maywood)* 228: 1–14, 2003.
11. **Fulton D, Gratton JP, McCabe TJ, Fontana J, Fujio Y, Walsh K, Franke TF, Papapetropoulos A, Sessa WC.** Regulation of endothelium-derived nitric oxide production by the protein kinase Akt. *Nature* 399: 597–601, 1999.
12. **Gammella E, Leuenberger C, Gassmann M, Ostergaard L.** Evidence of synergistic/additive effects of sildenafil and erythropoietin in enhancing survival and migration of hypoxic endothelial cells. *Am J Physiol Lung Cell Mol Physiol* 304: L230–L239, 2013.
13. **Giaid A, Saleh D.** Reduced expression of endothelial nitric oxide synthase in the lungs of patients with pulmonary hypertension. *N Engl J Med* 333: 214–221, 1995.
14. **Girgis RE, Champion HC, Diette GB, Johns RA, Permutt S, Sylvester JT.** Decreased exhaled nitric oxide in pulmonary arterial hypertension: response to bosentan therapy. *Am J Respir Crit Care Med* 172: 352–357, 2005.
15. **Higenbottam TW, Laude EA.** Endothelial dysfunction providing the basis for the treatment of pulmonary hypertension: Giles F. Filley lecture. *Chest* 114: 72S–79S, 1998.
16. **Homma N, Morio Y, Takahashi H, Yamamoto A, Suzuki T, Sato K, Muramatsu M, Fukuchi Y.** Genistein, a phytoestrogen, attenuates monocrotaline-induced pulmonary hypertension. *Respiration* 73: 105–112, 2006.
17. **Imagawa S, Tarumoto T, Suzuki N, Mukai HY, Hasegawa Y, Higuchi M, Neichi T, Ozawa K, Yamamoto M, Nagasawa T.** L-Arginine rescues

decreased erythropoietin gene expression by stimulating GATA-2 with L-NMMA. *Kidney Int* 61: 396–404, 2002.

18. **Karamsetty MR, Klinger JR, Hill NS.** Phytoestrogens restore nitric oxide-mediated relaxation in isolated pulmonary arteries from chronically hypoxic rats. *J Pharmacol Exp Ther* 297: 968–974, 2001.
19. **Karamsetty VS, MacLean MR, McCulloch KM, Kane KA, Wadsworth RM.** Hypoxic constrictor response in the isolated pulmonary artery from chronically hypoxic rats. *Respir Physiol* 105: 85–93, 1996.
20. **Lang M, Kojonazarov B, Tian X, Kalymbetov A, Weissmann N, Grimminger F, Kretschmer A, Stasch JP, Seeger W, Ghofrani HA, Schermuly RT.** The soluble guanylate cyclase stimulator riociguat ameliorates pulmonary hypertension induced by hypoxia and SU5416 in rats. *PLoS One* 7: e43433, 2012.
21. **Le Cras TD, McMurtry IF.** Nitric oxide production in the hypoxic lung. *Am J Physiol Lung Cell Mol Physiol* 280: L575–L582, 2001.
22. **Lipsic E, Schoemaker RG, van der Meer P, Voors AA, van Veldhuisen DJ, van Gilst WH.** Protective effects of erythropoietin in cardiac ischemia: from bench to bedside. *J Am Coll Cardiol* 48: 2161–2167, 2006.
23. **Marzo F, Lavorgna A, Coluzzi G, Santucci E, Tarantino F, Rio T, Conti E, Autore C, Agati L, Andreotti F.** Erythropoietin in heart and vessels: focus on transcription and signalling pathways. *J Thromb Thrombolysis* 26: 183–187, 2008.
24. **Morio Y, McMurtry IF.** Ca(2+) release from ryanodine-sensitive store contributes to mechanism of hypoxic vasoconstriction in rat lungs. *J Appl Physiol* 92: 527–534, 2002.
25. **Muramatsu M, Oka M, Morio Y, Soma S, Takahashi H, Fukuchi Y.** Chronic hypoxia augments endothelin-B receptor-mediated vasodilation in isolated perfused rat lungs. *Am J Physiol Lung Cell Mol Physiol* 276: L358–L364, 1999.
26. **Ohigashi T, Brookins J, Fisher JW.** Interaction of nitric oxide and cyclic guanosine 3=,5=-monophosphate in erythropoietin production. *J Clin Invest* 92: 1587–1591, 1993.
27. **Oka M, Morris KG, McMurtry IF.** NIP-121 is more effective than nifedipine in acutely reversing chronic pulmonary hypertension. *J Appl Physiol* 75: 1075–1080, 1993.
28. **Ou J, Fontana JT, Ou Z, Jones DW, Ackerman AW, Oldham KT, Yu J, Sessa WC, Pritchard KA.** Heat shock protein 90 and tyrosine kinase regulate eNOS NO* generation but not NO* bioactivity. *Am J Physiol Heart Circ Physiol* 286: H561–H569, 2004.
29. **Ou ZJ, Wei W, Huang DD, Luo W, Luo D, Wang ZP, Zhang X, Ou JS.** L-Arginine restores endothelial nitric oxide synthase-coupled activity and attenuates monocrotaline-induced pulmonary artery hypertension in rats. *Am J Physiol Endocrinol Metab* 298: E1131–E1139, 2010.
30. **Petit RD, Warburton RR, Ou LC, Brinck-Johnson T, Hill NS.** Exogenous erythropoietin fails to augment hypoxic pulmonary hypertension in rats. *Respir Physiol* 91: 271–282, 1993.
31. **Petit RD, Warburton RR, Ou LC, Hill NS.** Pulmonary vascular adaptations to augmented polycythemia during chronic hypoxia. *J Appl Physiol* 79: 229–235, 1995.

31a. **Räthel TR, Leikert JF, Vollmar AM, Dirsch VM.** The soy isoflavone genistein induces a late but sustained activation of the endothelial nitric oxide-synthase system in vitro. *Br J Pharmacol* 144: 394–399, 2005.

32. **Rounds S, Hill NS.** Pulmonary hypertensive diseases. *Chest* 85: 397–405, 1984.
33. **Rowland I, Faughnan M, Hoey L, Wähälä K, Williamson G, Cassidy A.** Bioavailability of phyto-oestrogens. *Br J Nutr* 89, *Suppl* 1: S45–S58, 2003.
34. **Ruschitzka FT, Wenger RH, Stallmach T, Quaschning T, de Wit C, Wagner K, Labugger R, Kelm M, Noll G, Rülicke T, Shaw S, Lindberg RL, Rodenwaldt B, Lutz H, Bauer C, Lüscher TF, Gassmann M.** Nitric oxide prevents cardiovascular disease and determines survival in polyglobulic mice overexpressing erythropoietin. *Proc Natl Acad Sci USA* 97: 11609–11613, 2000.
36. **Sato K, Morio Y, Morris KG, Rodman DM, McMurtry IF.** Mechanism of hypoxic pulmonary vasoconstriction involves ET(A) receptor-mediated inhibition of K(ATP) channel. *Am J Physiol Lung Cell Mol Physiol* 278: L434–L442, 2000.
37. **Satoh K, Fukumoto Y, Nakano M, Kagaya Y, Shimokawa H.** Emergence of the erythropoietin/erythropoietin receptor system as a novel cardiovascular therapeutic target. *J Cardiovasc Pharmacol* 58: 570–574, 2011.
38. **Satoh K, Kagaya Y, Nakano M, Ito Y, Ohta J, Tada H, Karibe A, Minegishi N, Suzuki N, Yamamoto M, Ono M, Watanabe J, Shirato K, Ishii N, Sugamura K, Shimokawa H.** Important role of endogenous erythropoietin system in recruitment of endothelial progenitor cells in hypoxia-induced pulmonary hypertension in mice. *Circulation* 113: 1442–1450, 2006.
39. **Shimoda LA, Sham JS, Sylvester JT.** Altered pulmonary vasoreactivity in the chronically hypoxic lung. *Physiol Res* 49: 549–560, 2000.
40. **Squadrito F, Altavilla D, Squadrito G, Saitta A, Cucinotta D, Minutoli L, Deodato B, Ferlito M, Campo GM, Bova A, Caputi AP.** Genistein supplementation and estrogen replacement therapy improve endothelial dysfunction induced by ovariectomy in rats. *Cardiovasc Res* 45: 454–462, 2000.
41. **Toma C, Jensen PE, Prieto D, Hughes A, Mulvany MJ, Aalkjaer C.** Effects of tyrosine kinase inhibitors on the contractility of rat mesenteric resistance arteries. *Br J Pharmacol* 114: 1266–1272, 1995.
42. **Ueno M, Seferynska I, Beckman B, Brookins J, Nakashima J, Fisher JW.** Enhanced erythropoietin secretion in hepatoblastoma cells in response to hypoxia. *Am J Physiol Cell Physiol* 257: C743–C749, 1989.
43. **Urao N, Okigaki M, Yamada H, Aadachi Y, Matsuno K, Matsui A, Matsunaga S, Tateishi K, Nomura T, Takahashi T, Tatsumi T, Matsubara H.** Erythropoietin-mobilized endothelial progenitors enhance reendothelialization via Akt-endothelial nitric oxide synthase activation and prevent neointimal hyperplasia. *Circ Res* 98: 1405–1413, 2006.
44. **van Albada ME, du Marchie Sarvaas GJ, Koster J, Houwertjes MC, Berger RM, Schoemaker RG.** Effects of erythropoietin on advanced pulmonary vascular remodelling. *Eur Respir J* 31: 126–134, 2008.
45. **Yang Y, Nie W, Yuan J, Zhang B, Wang Z, Wu Z, Guo Y.** Genistein activates endothelial nitric oxide synthase in broiler pulmonary arterial endothelial cells by an Akt-dependent mechanism. *Exp Mol Med* 42: 768–776, 2010.

Histopathology

Histopathology 2014, 65, 100–110. DOI: 10.1111/his.12368

Characterization of pulmonary cysts in Birt–Hogg–Dubé syndrome: histopathological and morphometric analysis of 229 pulmonary cysts from 50 unrelated patients

Toshio Kumasaka,[1,2] Takuo Hayashi,[2,3] Keiko Mitani,[2,3] Hideyuki Kataoka,[2,4] Mika Kikkawa,[2,5] Kazunori Tobino,[2,6] Etsuko Kobayashi,[2,7] Yoko Gunji,[2,7] Makiko Kunogi,[2,7] Masatoshi Kurihara[2,4] & Kuniaki Seyama[2,7]

[1]*Department of Pathology, Japanese Red Cross Medical Centre, Tokyo, Japan,* [2]*The Study Group of Pneumothorax and Cystic Lung Diseases, Tokyo, Japan,* [3]*Division of Human Pathology, Juntendo University Faculty of Medicine and Graduate School of Medicine, Tokyo, Japan,* [4]*Pneumothorax Centre, Tamagawa Hospital, Tokyo, Japan,* [5]*Division of Molecular and Biochemical Research, Biomedical Research Centre, Juntendo University Faculty of Medicine and Graduate School of Medicine, Tokyo, Japan,* [6]*Department of Respiratory Medicine, Iizuka Hospital, Fukuoka, Japan, and* [7]*Division of Respiratory Medicine, Juntendo University Faculty of Medicine and Graduate School of Medicine, Tokyo, Japan*

Date of submission 12 August 2013
Accepted for publication 4 January 2014
Published online *Article Accepted* 7 January 2014

Kumasaka T, Hayashi T, Mitani K, Kataoka H, Kikkawa M, Tobino K, Kobayashi E, Gunji Y, Kunogi M, Kurihara M, Seyama K

(2014) *Histopathology* 65, 100–110

Characterization of pulmonary cysts in Birt–Hogg–Dubé syndrome: histopathological and morphometric analysis of 229 pulmonary cysts from 50 unrelated patients

Aims: To characterize the pathological features of pulmonary cysts, and to elucidate the possible mechanism of cyst formation in the lungs of patients with Birt–Hogg–Dubé syndrome (BHDS), a tumour suppressor gene syndrome, using histological and morphometric analyses.

Methods and results: We evaluated 229 lung cysts from 50 patients with BHDS and 117 from 34 patients with primary spontaneous pneumothorax (PSP) for their number, size, location and absence or presence of inflammation. The BHDS cysts abutted on interlobular septa (88.2%) and had intracystic septa (13.6%) or protruding venules (39.5%) without cell proliferation or inflammation. The frequencies of these histological characteristics differed significantly from those seen in the lungs of patients with PSP ($P < 0.05$). Although the intrapulmonary BHDS cysts were smaller than the subpleural BHDS cysts ($P < 0.001$), there was no difference in size between them when there was no inflammation. The number of cysts diminished logarithmically and the proportion of cysts with inflammation increased as their individual sizes became greater ($P < 0.05$).

Conclusions: These results imply that the BHDS cysts are likely to develop in the periacinar region, an anatomically weak site in a primary lobule, where alveoli attach to connective tissue septa. We hypothesize that the BHDS cysts possibly expand in size as the alveolar walls disappear at the alveolar-septal junction, and grow even larger when several cysts fuse.

Keywords: alveolar-septal junction, cell–matrix interaction, folliculin, mechanical stresses, TGF-β

Address for correspondence: T Kumasaka, MD, Department of Pathology, Japanese Red Cross Medical Centre, 4-1-22, Hiro-o, Shibuya-ku, Tokyo 150-8935, Japan. e-mail: kumasaka_toshio@med.jrc.or.jp

Introduction

Birt–Hogg–Dubé syndrome (BHDS) is an autosomal dominant disorder characterized by hamartomas of the hair follicle, renal tumours, and multiple lung

© 2014 The Authors. *Histopathology* Published by John Wiley & Sons Ltd.
This is an open access article under the terms of the Creative Commons Attribution-NonCommercial-NoDerivs License, which permits use and distribution in any medium, provided the original work is properly cited, the use is non-commercial and no modifications or adaptations are made.

cysts accompanying spontaneous recurrent pneumothorax.[1] The *FLCN* gene responsible for BHDS was cloned in 2002,[2] but the function of folliculin, the protein encoded by *FLCN*, is not completely clear. Several studies have shown that the function of folliculin-binding proteins (FNIP1 and FNIP2) involves 5′-AMP-activated protein kinase (AMPK) and the mammalian target of rapamycin (mTOR) pathway, and that a complete loss of folliculin function leads to BHDS-associated tumorigenesis through dysregulation of AMPK and the mTOR pathway.[3–8]

Clinically, approximately 85% of BHDS patients have fibrofolliculoma diagnosed by histological testing of skin or lung cysts detected by CT imaging of the chest; additionally, 29–34% of these patients have renal tumours visible by CT imaging.[1,9] On molecular analysis, BHDS-associated renal tumours have a somatic mutation of a second copy of *FLCN*,[10] whereas fibrofolliculomas of BHDS patients do not necessarily have *FLCN* loss of heterozygosity (LOH), indicating that haploinsufficiency of *FLCN* leads to tumour-like lesions of the hair follicle.[11] In contrast to the kidney and skin lesions, neither tumour formation nor proliferation of abnormal cells has ever been reported as a feature of the pulmonary manifestations, for which multiple cysts constitute the sole abnormality in both radiological and pathological studies. In addition, as for fibrofolliculomas, the high penetrance of lung cysts[11,12] may indicate that the latter occur through haploinsufficiency of *FLCN*, and that LOH analysis of cysts is not as useful as it is for renal tumours and fibrofolliculomas.

The mechanism of cyst formation in BHDS is not well understood. Therefore, we believe that it is necessary to define the histopathological findings for these cysts and underlying parenchyma from a large number of BHDS patients. Previously, in lung specimens from such patients, bullae or blebs were found with underlying emphysematous changes,[13–15] thin-walled cysts were surrounded by normal parenchyma,[16–18] or the cysts showed a predominance of type II pneumocyte-like cuboidal cells.[4] However, the number of BHDS patients examined in these studies was small, and the focus might have been on pleural or subpleural cysts, the pathological findings for which would be significantly influenced by pneumothorax and pneumothorax-associated inflammation.

Here, we report the histological and morphometric characteristics of 229 lung cysts from 50 patients with BHDS, the largest cohort ever included in an investigation of the lung pathology of this disorder.

Materials and methods

Lung specimens were obtained from 50 Asian patients (49 Japanese and one Chinese) with BHDS from the archives or consultation files in the Pneumothorax Centre, Tamagawa Hospital, and Division of Respiratory Medicine, Juntendo University Faculty of Medicine and Graduate School of Medicine (Table 1). BHDS was diagnosed by the use of *FLCN* genetic tests, as described previously.[19,20] The age (median) at operation in the 50 patients was 38.5 years, ranging from 24 to 66 years (38 years, ranging from 27 to 50 years, in 19 men; 41 years, ranging from 24 to 66 years, in 31 women) (Table 1). Thirteen patients were smokers, four were ex-smokers, 30 had never smoked, and three lacked any documented smoking history. A total of 229 lung cysts (79 in men; 150 in women) were identified in the 350 tissue sections that we examined.

Lung tissues were obtained using video-assisted thoracic surgery (VATS), undertaken for the treatment of pneumothorax or for the diagnosis of cystic lung diseases, and were then appropriately inflated, and fixed with 10% buffered formaldehyde. After routine preparation, the formalin-fixed paraffin-embedded tissues were sectioned and stained with haematoxylin and eosin and Elastica–Masson trichrome (EM) or Elastica–Van Gieson (EVG) stains. We evaluated chronic inflammation in each cyst on low-power magnification (×4 objective lens attached to a BX51 microscope; Olympus, Tokyo, Japan): the presence of cellular inflammation was defined as the accumulation of lymphocytes or plasma cells; the presence of fibrous inflammation was defined by the presence of dense (sub)pleural scars and/or fibrotic lung tissue with replacement of architecture.[21] We measured the maximum diameter of each cyst on the sections stained with EM or EVG by using the ocular micrometer on a microscope (U-OCM10/100; Olympus) or micrometer callipers on a glass slide (Shinwa, Nagoya, Japan).

As a control for the analysis of pulmonary cysts, lung tissues were used from 34 Japanese patients presenting with primary spontaneous pneumothorax (PSP) to the Japanese Red Cross Medical Centre. The median age of these 34 patients was 24 years, ranging from 18 to 30 years (33 men, and one woman aged 25 years). All of the 117 cysts associated with PSP were diagnosed as bullae and/or blebs.

Statistical analysis was performed using the Mann–Whitney *U*-test and χ^2-test (STATMATE III for Windows; ATMS, Tokyo, Japan), or the Kruskal–Wallis test (IBM SPSS STATISTICS; IBM Japan, Tokyo, Japan). A

Table 1. Summary of Birt–Hogg–Dubé syndrome cases

No	Age (years)	Sex	Smoking history	Location	*FLCN* mutation	No. of tissue sections	No. of cysts	Other findings
1	38	M	S	Exon 4	c.119delG	7	2	
2	38	F	S	Exon 5	c.328C>T	1	1	
3	38	F	S	Intron 5	c.396 + 1G>A	3	3	
4	29	M	N	Intron 5	c.397-2A>C	8	1	
5	36	F	U	Exon 6	c.397-13_397-4delGGCCCTCCAG	1	3	
6	37	F	U	Exon 6	c.402delC	2	3	
7	39	F	S	Exon 7	c.769_771delTCC	7	8	
8	40	F	N	Exon 7	c.769_771delTCC	9	8	
9	47	F	N	Exon 8	c.853C>T	7	1	Fibrosis
10	38	F	N	Exon 9	c.889_890delGA	7	5	
12	48	F	N	Exon 9	c.932_933delCT	6	3	
11	44	F	N	Exon 9	c.991_992dupTC	10	11	
13	48	M	N	Exon 9	c.997_998delTC	8	4	
14	34	M	S	Intron 9	c.1063-2A>G	8	8	Emphysema
15	53	F	N	Exon 10	c.1063-10_1065delTCTTGTTTAGGTC	5	6	
16	24	F	S	Exon 11	c.1285dupC	6	1	
17	29	M	S	Exon 11	c.1285dupC	4	2	
18	33	F	N	Exon 11	c.1285dupC	7	1	Granuloma
19	35	F	S	Exon 11	c.1285dupC	7	13	
20	35	M	N	Exon 11	c.1285dupC	3	1	
21	38	M	S	Exon 11	c.1285dupC	5	3	
22	39	M	S	Exon 11	c.1285dupC	12	6	
23	41	F	N	Exon 11	c.1285dupC	20	9	
24	43	F	N	Exon 11	c.1285dupC	4	8	
25	47	F	N	Exon 11	c.1285dupC	6	1	
26	50	M	N	Exon 11	c.1285dupC	10	6	
27	62	F	N	Exon 11	c.1285dupC	4	1	
28	64	F	S	Exon 11	c.1285dupC	24	15	Granuloma
29	31	F	N	Exon 12	c.1347_1353dupCCACCCT	5	4	
30	32	M	U	Exon 12	c.1347_1353dupCCACCCT	3	7	

Table 1. (Continued)

No	Age (years)	Sex	Smoking history	Location	*FLCN* mutation	No. of tissue sections	No. of cysts	Other findings
31	38	F	N	Exon 12	c.1347_1353dupCCACCCT	15	5	
32	42	F	S	Exon 12	c.1347_1353dupCCACCCT	7	8	
33	43	F	S	Exon 12	c.1347_1353dupCCACCCT	7	5	
34	43	F	N	Exon 12	c.1347_1353dupCCACCCT	5	6	
35	45	F	N	Exon 12	c.1347_1353dupCCACCCT	8	4	
36	48	M	S	Exon 12	c.1347_1353dupCCACCCT	6	4	
37	57	F	N	Exon 12	c.1347_1353dupCCACCCT	5	4	
38	66	F	N	Exon 12	c.1347_1353dupCCACCCT	4	2	Emphysema
39	46	M	N	Exon 12	c.1429C>T	5	2	
40	32	F	N	Intron 12	c.1433-1G>T	8	7	
46	43	M	N	Exon 13	c.1489_1490delGT	4	1	
41	26	F	S	Exon 13	c.1533_1536delGATG	1	1	
42	27	M	S	Exon 13	c.1533_1536delGATG	5	1	
43	34	M	N	Exon 13	c.1533_1536delGATA	15	6	
44	35	M	S	Exon 13	c.1533_1536delGATG	21	8	
45	38	M	N	Exon 13	c.1533_1536delGATG	4	3	
47	29	M	N	Exon 14	c.1539-?_c.1740 + ?del	8	8	
48	46	M	N	Exon 14	c.1539-?_c.1740 + ?del	6	6	
49	31	F	N	Exons 9–14	c.872-?_c.1740 + ?del	6	2	
50	58	F	N	Exons 9–14	c.872-?_c.1740 + ?del	1	1	

N, never smoker; S, current smoker; U, unknown.

P-value of <0.05 was considered to be statistically significant. This study was approved by the ethical committee in Juntendo University School of Medicine (No. 17053) and by the ethical committee for clinical studies in the Japanese Red Cross Medical Centre (No. 429).

Results

HISTOLOGICAL CHARACTERISTICS

The lung tissues obtained from 45 of 50 patients with BHDS had normal parenchyma, whereas those from the other five had centrilobular emphysema (two patients), granulomas (two patients) or fibrosis (one patient) in the parenchyma (Table 1, and data not shown). Macroscopic findings demonstrated that the lung cysts, which occasionally contained intracystic septa, had very thin and translucent walls, and were surrounded by normal lung parenchyma in all patients (Figure 1A and B). The intracystic septa seen in 13.6% of BHDS cysts were composed of interlobular septa, and venules protruding into the cyst (observed in 39.5% of BHDS cysts) sometimes showed regression of surrounding connective tissue (Figure 1C). The anatomical and histological findings were characterized by the following features (Table 2). Half of the lung cysts were located in the subpleural area (Figure 1D), and the remainder in the intrapulmonary area (Figure 1E); the cysts abutted on interlobular septa but rarely on bronchioles. The BHDS cysts, especially those located in lung

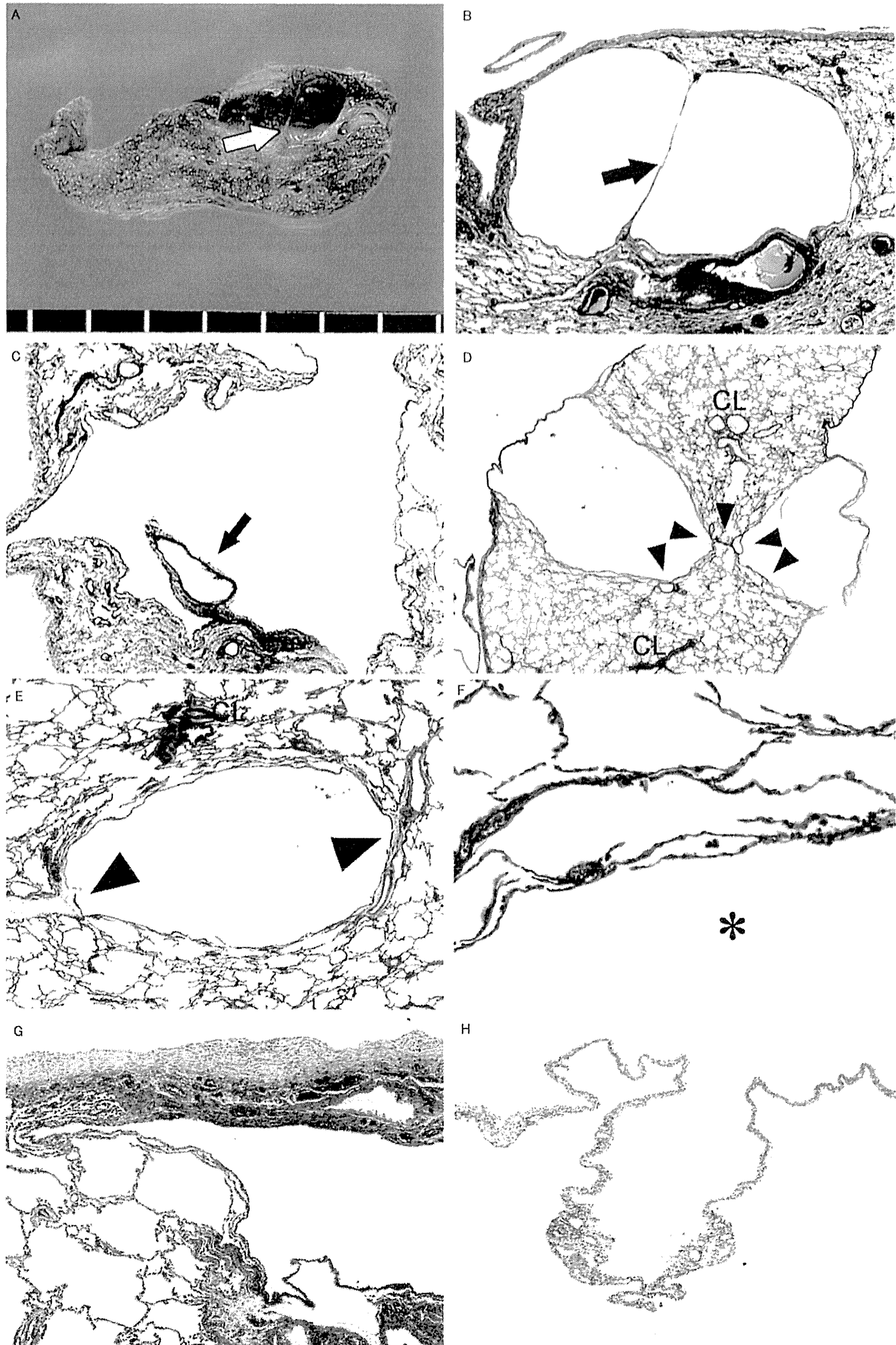
A
B
C
D
CL
CL
E
CL
F
*
G
H

Figure 1. Representative pathological findings of pulmonary cysts from patients with Birt–Hogg–Dubé syndrome (BHDS). A, A cyst in the subpleural area has, macroscopically, a very thin, translucent wall with an intracystic septum indicated by a white arrow (scale bar: 5 mm). B, The cyst shown in A was located in the area adjacent to an interlobular septum including pulmonary veins, and has a very thin intracystic septum (indicated by the black arrow) (Elastica–Masson trichrome stain). C, Vessels in the interlobular septa frequently protrude into the cyst. Note that the connective tissue surrounding one of the of the vessels is decreased (indicated by a small black arrow) (Elastica–Masson trichrome stain). D, Two subpleural cysts abut on an interlobular septum (small arrowheads), and the opposite side of each cyst wall is composed of thin pleural wall (CL indicates a centrilobular area). E, An intrapulmonary cyst abuts on an interlobular septum (large arrowheads), and the other side of the cyst wall is composed of thin alveolar wall (CL indicates a centrilobular area.). F, Approximately half of all cysts that we examined in this study were composed of normal alveolar walls with neither cell proliferation nor inflammatory cell infiltrates (* indicates intracystic area). However, some cysts from BHDS have inflammation, and representative photomicrographs of subpleural cysts are presented in G and H. In G, the basal side of a subpleural cyst abuts on an interlobular septum without inflammation, whereas its pleural side shows thickened visceral pleura with fibroblast proliferation. In H, the very thin wall of a subpleural cyst shows but lymphocyte infiltration but no fibrous thickening.

parenchyma, were not at all or little affected by inflammation, including fibrosis (Figure 1F), although approximately one-third of subpleural cysts showed mild inflammation, including fibroblast proliferation (Figure 1G) and lymphocyte infiltration (Figure 1H). The pulmonary cysts of BHDS patients showed far more clearly defined pathological features than the pulmonary cysts (bullae or blebs) of PSP patients, and differences were statistically significant (Table 2). In BHDS patients: (i) cysts were present in both subpleural and intrapulmonary areas; (ii) cysts frequently abutted on interlobular septa, often had venules protruding into the cyst, and occasionally accompanied intracystic septa, suggesting the periacinar development of cysts in a primary lobule; and (iii) cysts usually had no sign of inflammation, especially those in intrapulmonary areas.

BHDS and PSP patients were then compared for the pathological features (inflammatory site and type) of subpleural cysts with inflammation (Figure 2). Most cysts from PSP patients were located in subpleural areas and had inflammatory infiltrates. Subpleural BHDS cysts that were inflamed were less likely to have such inflammation (especially of the fibrous type) at a basal site (i.e. proximal part of a subpleural cyst) (Table 3). The most prominent feature of subpleural BHDS cysts that distinguished them from PSP cysts was the former's almost complete absence of fibrous inflammation in the basal area, with 94.8% sensitivity and 92.2% specificity.

Table 2. Comparison of the numbers of cysts in lung specimens from patients with Birt–Hogg–Dubé syndrome (BHDS) and primary spontaneous pneumothorax (PSP) [no. (%)]

Histological findings	Cysts from BHDS patients (n = 229)	Cysts from PSP patients (n = 117)	χ^2 -test
Cysts located in			
Subpleural area	116 (50.7)	115 (98.3)	$P < 0.001$
Intrapulmonary area	113 (49.3)	2 (1.7)	
Cysts abutting on			
Interlobular septa	202 (88.2)	16 (13.7)	$P < 0.001$
Bronchiole	11 (4.8)	42 (35.9)	$P < 0.001$
Intracystic septa	31 (13.6)	0 (0)	$P < 0.001$
Venules protruding into the cyst	90 (39.5)	2 (1.7)	$P < 0.001$
Cysts without inflammation			
Total	125/229 (54.6)	2/117 (1.7)	$P < 0.001$
Subpleural area	37/116 (31.9)	2/115 (1.7)	$P < 0.001$
Intrapulmonary area	88/113 (77.9)*	0/2 (0)	NS ($P = 0.177$)

*$P < 0.001$ for comparison of the numbers of cysts without inflammation between the subpleural and intrapulmonary areas.

NS, not significant.

© 2014 The Authors. *Histopathology* Published by John Wiley & Sons Ltd.

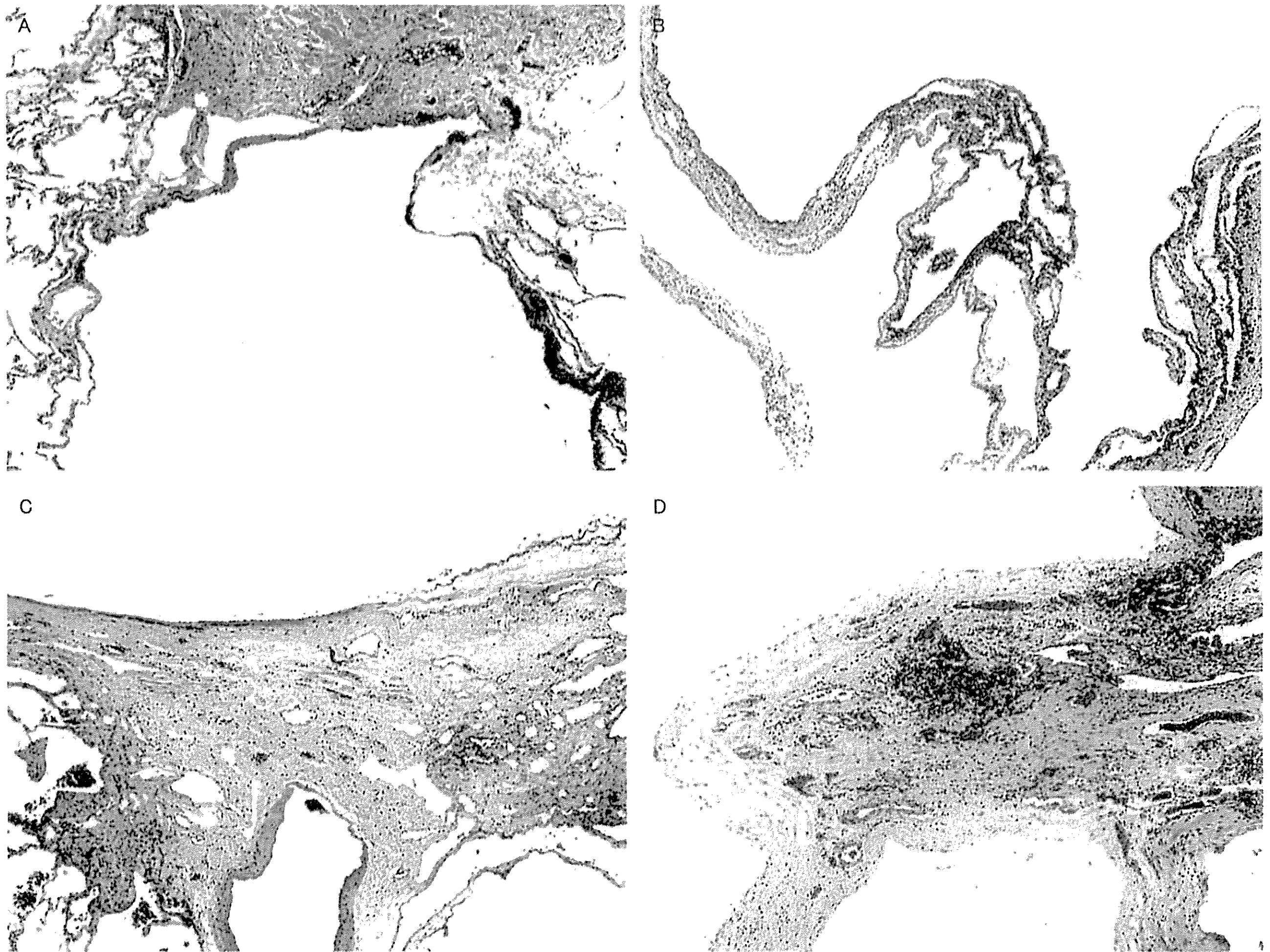

Figure 2. Representative photomicrographs showing cyst-associated cellular and/or fibrous inflammation: A, no inflammation (from an intrapulmonary cyst in Birt–Hogg–Dubé syndrome, BHDS: note that the cyst abuts on an interlobular septum in the upper area); B, cellular inflammation (from a subpleural cyst in BHDS); C, fibrous inflammation (from bullae in primary spontaneous pneumothorax, PSP); and D, cellular and fibrous inflammation (from bullae in PSP).

MORPHOMETRIC ANALYSIS

We examined the histological features of cysts in terms of size and location in the lung parenchyma. The maximum diameter of cysts associated with BHDS ranged from 1.0 to 15.7 mm (median: 3.8 mm), and two-thirds of them had diameters of ≤5 mm. A histogram depicting our analysis of size shows that the number of the cysts logarithmically diminished as the maximum cyst size increased [correlation coefficient for the fitted curve, $y = -23.3 \ln(x) + 63.0$, $R^2 = 0.925$] (Figure 3). In addition, the proportion of cysts with inflammation increased as the maximum cyst size increased. However, no significant difference was noted in maximal cyst size between men and women [median 4.0 mm (range 1–15.7 mm) versus 3.5 mm (range 1.0–13.2 mm), $P = 0.6908$] or between patients with or without a history of smoking [median 4.0 mm (range 1.0–12.6 mm) versus 3.4 mm (range 1.0–15.7), $P = 0.1508$]. Statistical significance was evident for the larger size of subpleural cysts than of intrapulmonary cysts [median 5.0 mm (range 1.0–15.7 mm) versus 3.0 mm (range 1.0–9.8 mm), $P < 0.0001$] and for the larger size of cysts with inflammation than of those without inflammation [median 4.7 mm (range 1.1–15.7 mm) versus 3.3 mm (range 1.0–9.8 mm), $P < 0.0001$]. When we evaluated the influence of location or inflammation on maximum cyst size, the results demonstrated that subpleural cysts with inflammation were significantly larger than those without inflammation. However, the size of in-

Table 3. Comparison of the numbers of subpleural cysts with inflammation in Birt–Hogg–Dubé syndrome (BHDS) and primary spontaneous pneumothorax (PSP). Inflammation was examined with regard to the location of the cyst (pleural or basal site) and type of inflammation (cellular or fibrous)

	No. of subpleural cysts examined	No. of cysts with inflammation (%)	Inflammation at pleural site, no. (%)		Inflammation at basal site, no. (%)	
			Cellular	Fibrous	Cellular	Fibrous
BHDS	116	79 (68.1)	75 (64.7)	55 (47.4)	19 (16.4)	6 (5.2)
PSP	115	115 (100)	73 (63.5)	115 (100)	56 (48.7)	106 (92.2)
χ^2– test		$P < 0.001$	$P = 0.852$	$P < 0.001$	$P < 0.001$	$P < 0.001$

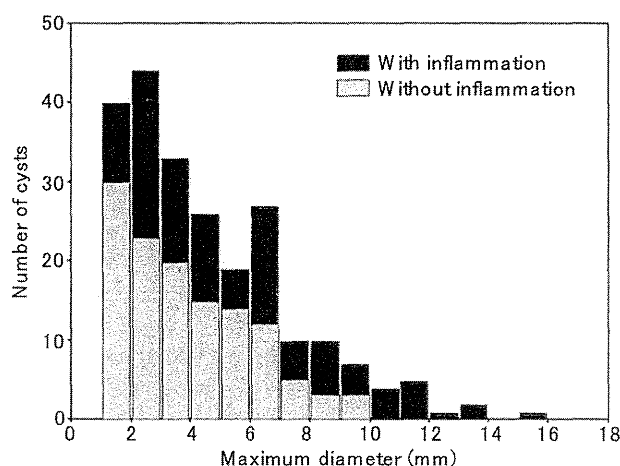

Figure 3. Distribution of the maximum diameter of pulmonary cysts in patients with Birt–Hogg–Dubé syndrome. Black and grey columns indicate the numbers of pulmonary cysts with and without inflammation, respectively.

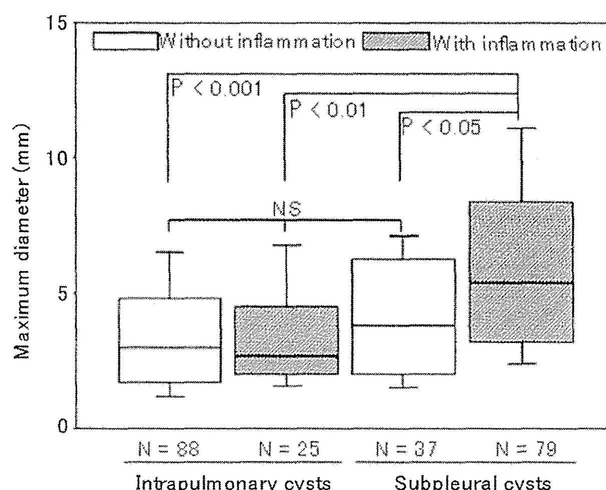

Figure 4. Comparison of the maximum diameters of intrapulmonary and subpleural cysts in patients with BHDS.

trapulmonary cysts was not affected by the presence or absence of inflammation, and the size of subpleural cysts without inflammation resembled that of non-inflamed intrapulmonary cysts (Figure 4).

Discussion

We have demonstrated the unique histological characteristics of pulmonary cysts from 50 unrelated patients with BHDS, the largest cohort ever included in a study of lung pathology focusing on BDHS. Our results show that pulmonary BHDS cysts are: (i) surrounded by normal alveolar walls; (ii) abut on interlobular septa; and (ii) may have intracystic septa and/or protrusion of venules into the cystic space, indicating disappearance of the surrounding alveolar wall and/or regression of connective tissue of interlobular septa. These histological characteristics can differentiate BHDS from other cystic lung diseases. For example, tuberous sclerosis complex (TSC)-associated lymphangioleiomyomatosis (LAM) always shows LAM cell proliferation in the cyst walls. In other hereditary cystic lung diseases, such as cystic fibrosis, Ehlers–Danlos syndrome, and Marfan syndrome, patients have non-specific cystic lesions with cellular or fibrous inflammation.[22–24] In the non-hereditary lung cystic diseases, including Langerhans cell histiocytosis, amyloidosis, Sjögren syndrome, and lymphocytic interstitial pneumonia, infiltration of inflammatory cells and/or matrix deposition always occurs.[25]

The present study clearly establishes that neither inflammation nor cell proliferation contributes to cyst formation in patients with BHDS, because most of their cysts, especially intrapulmonary BHDS cysts that do not suffer from the secondary effects of pneumothorax, show neither inflammation nor abnormal cell proliferation. As the majority of BHDS cysts are

located far from bronchioles, the mechanism for cyst formation in BHDS is less likely to be associated with a check-valve mechanism, which is supposedly operative on cyst formation in PSP, smoking-related diseases, Sjögren syndrome, and other non-hereditary cystic lung diseases. We have demonstrated in the present study that most of the intrapulmonary BHDS cysts (88/113, 77.9%) lack inflammation, whereas only approximately one-third of the subpleural cysts (37/116, 31.9%) have no inflammation (Table 2). Accordingly, we think that most, if not all, of the inflammatory changes observed were associated with pneumothorax. It has already been well described that pneumothorax causes pleural inflammation at the pleural side of the cyst, but not at the basal side.[26] In addition, an animal experiment clearly showed that repeated injection of air into the pleural space caused inflammation and the formation of 'neomembranes' composed of fibroblasts and collagen that was variably covered by proliferation of mesothelial cells.[27] In addition, the finding that the BHDS cysts without inflammation had no significant difference in size, irrespective of whether they were subpleural or intrapulmonary (Figure 4), suggests that inflammation secondary to pneumothorax is likely to contribute to the subsequent growth of subpleural cysts in BHDS. Interestingly, we have demonstrated a logarithmic decline in the number of cysts as the size of individual cysts increases. Possibly, the fusion of small cysts resulted in the enlargement that we noted. This process may also explain how intracystic septa develop in BHDS cysts, as abutting cysts could fuse with intervening interlobular septa. In this context, the protrusion of venules into ~40% of the BHDS cysts may have been caused not only by the disappearance of alveolar walls adjoining interlobular septa, but also by regression of their surrounding connective tissue in the septa.

The mechanism for development of pulmonary cysts in BHDS has been discussed in several reports. Graham *et al.*[14] speculated that a genetic abnormality was responsible for postnatal alveolar proliferation of the peripheral lung, on the basis of pathological examination of three BHDS non-smokers, as they found cysts predominantly in the subpleural area. Warren *et al.*[28] found that *FLCN* was expressed in type I pneumocytes and stromal cells, including fibroblasts and macrophages in the lungs, and hence proposed a possible role for functional abnormalities of these folliculin-expressing cells in cyst formation. Recently, Furuya *et al.*[4] reported that dysregulation of the mTOR pathway resulting from haploinsufficiency of *FLCN* may induce cyst formation through proliferation of type II pneumocytes. However, the above mechanisms were deduced from an examination of limited numbers of lung specimens, and are therefore unlikely to fit the histopathological features of BHDS cysts and lungs defined after detailed analysis of the much larger specimen sample presented here. For example, cysts are present not only in subpleural areas but also in parenchyma, and most cysts have neither cellular proliferation nor inflammation, especially cysts in the parenchymal area, where secondary changes resulting from pneumothorax would not affect the pathological findings, in contrast to cysts at subpleural sites. In addition, when bullae/blebs are affected by pneumothorax, they will usually have reactive proliferation of type II pneumocytes. If proliferation of type II pneumocytes were actively involved in cyst formation, those cysts would show no predilection for the location and distribution recorded here; instead, they should be detectable not only in the area surrounded by interlobular septa, but also in the centrilobular area. Furthermore, one would expect cyst formation to proceed by proteolysis, as in smoke-related inflammatory diseases, collagen diseases, and neoplastic diseases such as LAM.[29] Otherwise, the proliferation of type II pneumocytes might form a lung tumour, like multifocal micronodular pneumocyte hyperplasia occurring via dysregulation of the mTOR pathway in patients with TSC.[18] However, in the present study, lung specimens from BHDS patients showed no destruction of lung architecture by either proliferating type II pneumocytes or inflammation, indicating that BHDS cysts may not develop through proliferation of type II pneumocytes or proteolysis mediated by proliferating type II pneumocytes.

Presumably, considering the unique histological characteristics of BHDS cysts defined by the present study, almost all cysts abutting on interlobular septa without significant inflammation should ensue naturally from the inherent mechanism of cyst formation. In this context, we postulate that *FLCN* mutation results in abnormalities at the alveolar-septal junction. Several reports have described folliculin, the protein encoded by *FLCN*, as a regulator of TGF-β signalling, especially TGF-β_2,[30] or cell–cell adhesion through the interaction with adherence junction protein.[31] TGF-β_2 is involved in epithelial–mesenchymal interactions, cell growth, the production of extracellular matrix proteins, and tissue remodelling during development or normal subepithelial matrix homeostasis.[32,33] Warren *et al.*[28] demonstrated that *FLCN* mRNA was strongly expressed in stromal cells within the connective tissue and weakly in type I

© 2014 The Authors. *Histopathology* Published by John Wiley & Sons Ltd,